Přírodovědecká fakulta
Faculty of Science

Jihočeská univerzita v Českých Budějovicích
University of South Bohemia in České Budějovice

OASL protein isoforms in human neural cell lines infected by tick-borne encephalitis

Bachelor's thesis

Anđa Radoš

Thesis Supervisor: RNDr. Ján Štěrba, Ph.D.

České Budějovice

2017

Radoš, A., 2017: OASL isoforms in human neural cell lines infected by tick-borne encephalitis. Bc. Thesis, in English. – 53 pp., Faculty of Science, University of South Bohemia, České Budějovice, Czech Republic.

Annotation

OASL is a protein found to play role in antiviral response. It is overexpressed in human cell lines upon infection with TBEV virus. OASL has three isoforms (OASL a, OASL b and OASL d). The aim of the thesis was the detection of OASL isoforms expression in TBEV-infected human brain cells (glioblastoma, medulloblastoma and neuroblastoma cell lines used) at different time intervals of infection. Detection was performed on mRNA level.

Affirmation

I hereby declare that I have worked on my [bachelor's dissertation] thesis independently and used only the sources listed in the bibliography. I hereby declare that, in accordance with Article 47b of Act No. 111/1998 in the valid wording, I agree with the publication of my bachelor / master / dissertation thesis, in full / in shortened form resulting from deletion of indicated parts to be kept in the Faculty of Science archive, in electronic form in publicly accessible part of the STAG database operated by the University of South Bohemia in České Budějovice accessible through its web pages. Further, I agree to the electronic publication of the comments of my supervisor and thesis opponents and the record of the proceedings and results of the thesis defence in accordance with aforementioned Act No. 111/1998. I also agree to the comparison of the text of my thesis with the Theses.cz thesis database operated by the National Registry of University Theses and a plagiarism detection system.

České Budějovice, Date ……

Anđa Radoš

Acknowledgements

I would like to thank to my supervisor, RNDr. Ján Štěrba, Ph.D. for giving me the opportunity to work with on this topic.

Special thanks goes to Mgr. Martin Selinger, my assistant supervisor, for all the support and knowledge he unselfishly shared with me, for guidance throughout this work and readiness and will to always help with everything.

I also want to express a great thankfulness and gratefulness to my family and friends, who provided me with a full-time support on every level. Special thanks goes to my sister, Danica Radoš, who was there when I needed her most.

Table of content

List of Abbreviations

TBEV - tick-borne encephalitis virus

NKV - viruses with no know vector

CNS - central nervous system

ER - endoplasmic reticulum

BBB - blood-brain barrier

HS - heparan sulfate

NCR - non-codin region

SVP - capsidless subviral particle

PRR - germline-encoded pattern-recognition receptor

PAMP - pathogen – associated molecular pattern

TLR - Toll-like receptors

RLR – RIG-like receptors

RIG – retinoic acid-inducible gene

LRR - leucine-rich-repeat

TIR - Toll/IL-1R homology

IL-1R – interleukin-1 receptor

MyD88 - myeloid differentiation factor 88

TRAM - translocating chain-associating membrane (TRAM) protein

IFN – interferon

dsRNA – double-stranded RNA

ssRNA – single-stranded RNA

poly I:C - polyinosine-deoxycytidylic acid

CARD - caspase recruitment domain

MDA5 - melanoma differentiation associated gene 5

OAS - oligoadenylate synthetases

ISG - IFN-stimulated gene

RNaseL - the latent form of RNase

OASL – OAS-like

UBL – ubiquitin - like

pUb - polyubiquitin

bp – base pair

MOI – multiplicity of infection

RT-PCR - reverse transcription-polymerase chain reaction

qRT-PCR - quantitative reverse transcription-polymerase chain reaction

cDNA – complementary DNA

1. Introduction

1.1 Tick-borne encephalitis virus (TBEV)

1.1.1 TBEV - epidemiology and transmission

Tick-borne encephalitis (TBE) represents neurological infection caused by the TBEV. The first descriptions of this virus originate from the 18th century in Finland. Later, in 1937 in Russia, Lev Zilber isolated the virus from the tick specie *Ixodes persulcatus* (Gritsun, Lashkevich, and Gould 2003).

TBEV belongs to the genus *Flavivirus* within the *Flaviviridae* family. Inside of *Flavivirus* genus, three groups of viruses exist: tick-borne viruses, mosquito-borne viruses and viruses with no know vector. The tick-borne flaviviruses are further divided into two groups: the mammalian group and the seabird group. TBEV belongs to the mammalian group and can be categorized into three subtypes: Western European or European (formerly noted as Central European encephalitis - CEE), Siberian (formerly West-Siberian) and Far Eastern (formerly noted as Russian spring-summer encephalitis - RSSE). Mammalian group comprises of viruses antigenically related to TBEV, including: Louping ill virus (LIV), Langat virus (LGTV), Powassan virus (POWV), Omsk hemorrahgic fever virus (OHFV), Kyasanur Forest disease virus (KFDV together with the recently recognized Alkhurma virus, ALKV considered as its subtype), Kadam virus (KADV), Royal Farm virus (RFV, together with its subtype Karshi virus), Gadgets Gully Virus (GGYV) (Gritsun, Lashkevich, and Gould 2003).

LIV and LGTV show close molecular relationships to TBEV but do not have that important role as disease agents on human organism. On the other side, in mammals they cause neurological illness similar to TBEV. Unlike these viruses, TBEV infects the central nervous system (CNS) in the human organism. In most cases TBEV is transmitted to humans *via* tick bite, however, in rare cases it could be transmitted *via* dairy products and unpasteurised milk of infected goat or sheep. In addition to this, several cases have been reported where infection was transmitted by needle-stick injury or from inhaling infected aerosol (Christian W. Mandl 2005).

1.1.2 Natural cycle of TBEV

TBEV circulates in the nature mostly between two species: one already mentioned - *Ixodes persulatus* (Siberian and Far-Eastern) and the other - *Ixodes ricinus* (Western Europe) (Mansfield et al. 2009). Some animal species, such as shrew mouse, mole and hedgehogs, can act as important reservoirs of the virus. However, several different species of rodents are amplifying hosts for the virus. When it comes to its transmission in nature, it can happen in two ways. One way is from infected female tick to its prodigy and it remains throughout the development stages from larvae to nymphs and later adults. Another way is related to feeding, whereby uninfected larvae or nymphs get infected if they co-feed next to infected tick but also if they eat on a viremic animal (Labuda et al. 1997). We could say that co-feeding is one of the most relevant pathways of viral spread between ticks. Reason for this lay is the fact that transmission can occur even if the viruses are not significantly present in the blood (viremia) and also on immune hosts. However, endemnicity requires horizontal transmission among ticks and vertebrates (Christian W. Mandl 2005).

Figure 1 (Donoso-Mantke et al., 2011) depicts life cycle of ixodid tick and transmission cycle of TBE virus.

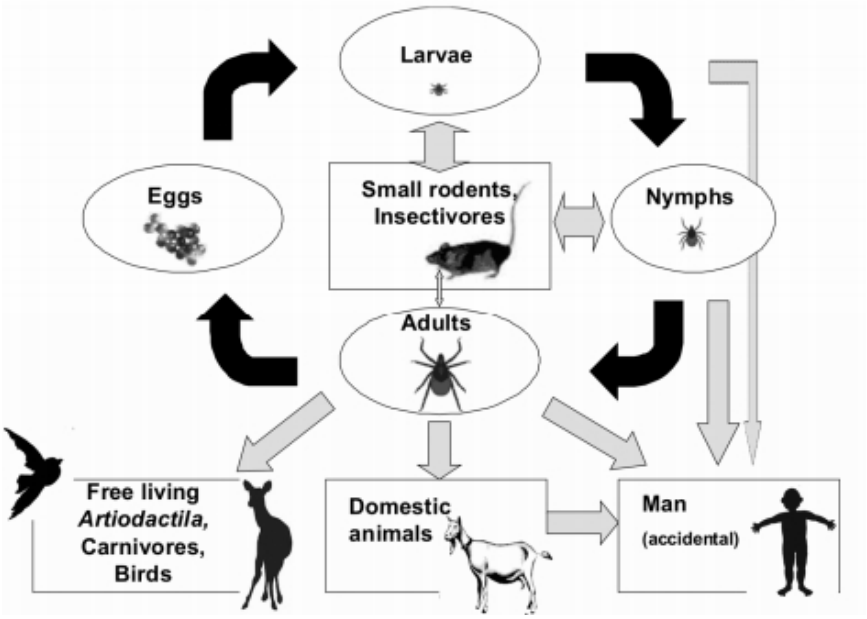

Figure 1: Life cycle of ixodid tick and transmission cycle of TBE virus: TBEV-infected female tick transmits the virus to its prodigy and the virus remains persistent in the tick throughout all four stages of its life cycle (egg, larvae, nymph and adult). Transmission of the virus from ticks to humans and small rodents is possible at any point of viral transstadial transmission (from larvae to nymphs to adult tick). Birds, carnivores and domestic animals get infected *via* adult tick's bite. TBEV can be transmitted from domestic animals to human *via* animal products (e.g. milk) (Donoso-Mantke et al., 2011).

1.1.3 Neuropathogenesis of TBEV

As already mentioned, humans get infected from the tick bite, but regardless of this, they are dead-end hosts for the virus as they do not have a role in its maintenance in nature. When it comes to the mechanism of infection after the bite, probably the first cells that get infected are epidermal Langerhans cells. Not only are they considered to be the first, but also the most important host cells to be influenced. After initial infection, Langerhans cells transport the virus to the draining lymph nodes and initiate the spread of infection to lymphoid compartments (Labuda et al. 1996). Systematic infection and viremia are caused by virus replication in these and other tissues. At the beginning, it was noted that TBEV affects the central nervous system, but it is still not clear how it ranges over the blood-brain barrier (BBB). One of the possible mechanisms proposed includes infection of human brain microvascular endothelial cells (HBMECs) which then multiply the virus and release it into the CNS, without compromising the BBB integrity. After this model, BBB breakdown represents a consequence of TBEV infection rather than a requirement for its entry into the brain (Palus et al. 2017). On the other hand, it is confirmed that the viral invasion of CNS requisite high-level viremia. Even though different CNS cell types can be infected, primary target are neurons (Kaiser 1999).

Figure 2 (Donoso-Mantke et al., 2011) depicts steps of TBE virus entry into human organs and tissues.

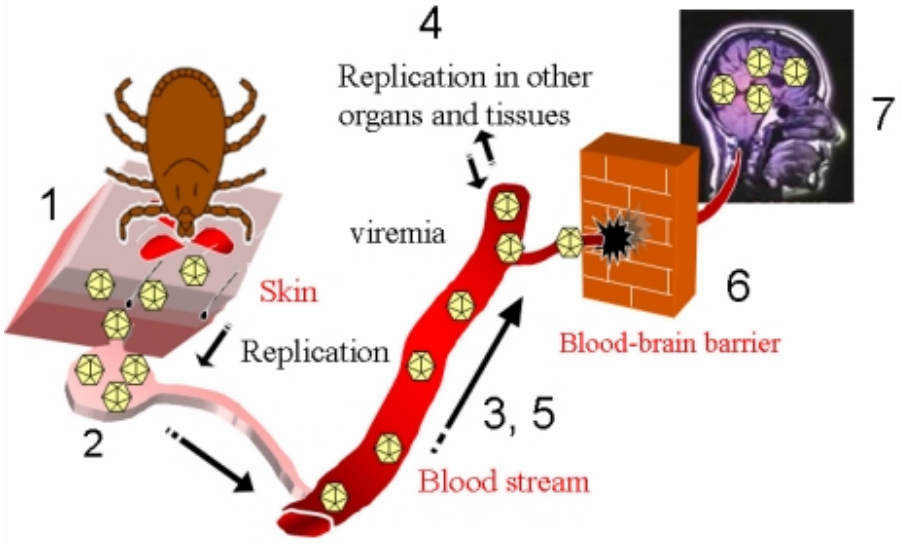

Figure 2: Schematic drawing of the steps during TBE virus infection: TBEV-infected tick transmits the TBE virus by its bite while feeding on humans (1). Viral particles start to replicate and enter the blood stream (2) *via* which they are carried to different tissues and organs (3) where they further replicate (4) and continue to circulate around the body carried by blood (5). In order for viruses to enter the human brain, (7) they first have to cross blood-brain barrier (6) and they do so by infection of endothelial cells (Donoso-Mantke et al., 2011).

Before TBEV affects the CNS, there are some developmental stages of this disease. During the incubation period, that lasts around 7-14 days, symptoms that appear can be a headache, pain in the shoulders, neck and in lower back, fatigue and this is accompanied by vomiting and high fever. Second phase occurs when the disease progresses to the neurological involvement and this period is known as asymptomatic (lasting time 2-10 days). Main symptoms of this second phase are high fever and acute CNS infection that can manifest in the spinal cord to cause myelitis, meninges where the inflammation causes meningitis, the nerve roots (radiculitis) or the brain parenchyma (can cause encephalitis). (Mansfield et al. 2009). For the first viremic phase of infection, reverse-transcriptase polymerase chain reaction (RT-PCR) can be used for diagnosis. When neurological symptoms occur, TBEV is usually diagnosed by serological methods, mostly enzyme-linked immunosorbent assay (ELISA). Within the sixth day of illness IgM antibodies appear, but early diagnosis of TBEV with these antibodies can be questionable. The reason for this is the fact that in certain vaccines or individuals who naturally obtain the infection, IgM antibodies can remain in the system for more than 9 months. In addition, response of IgM antibodies can be delayed or weak (Mansfield et al. 2009).

When it comes to curing the TBE, there is no specific curative therapy. Usually supportive treatments are used and they include nonsteroidal anti-inflammatory drugs, paracetamol or aspirin. In some severe cases, patients are given corticosteroids even though their use has not been validated. Furthermore, the main prevention of TBE disease is vaccination and they are effective and safe between 95% and 99% (Mansfield et al. 2009).

Virus possess two distinct properties that enable neuropathogenesis of TBEV - neuroinvasiveness and neurovirulence. The first one refers to virus' capacity to enter the CNS, and the latter to its replicating capacity and capability to cause damage in the CNS (especially in neurons). Neuropatogenicity of TBEV strains and mutants can be examined with a number of animal models. Unlike wild animals, that are not susceptible to TBEV induced disease, most of laboratory mice are and that is the main reason why they are often used as a model for research. When mice are inoculated with living virus, fatal infection of the CNS occurs with neurological symptoms that are similar to the acute TBE condition in humans. Results of this research showed that strains genetically mapped to a mutation in the 2'-5' - oligoadenylate synthetase gene OAS 1b (OAS proteins are discussed in later chapters), a member of an interferon-inducible protein family that plays an important role in the endogenous antiviral family (Brinton and Perelygin 2003; Mashimo et al. 2002; Perelygin et al. 2002). Intracranial inoculation of the virus into juvenile or suckling mouse

serves for examination of neurovirulence in the animal model, whereas peripheral (subcutaneous or intraperitoneal) inoculation into juvenile or adult mice provides analyses of neuroinvasiveness. TBEV wild-type strains are neuropathogenic in both inoculation methods, intracranial and peripheral, and generate lethal CNS infections. It is important to emphasize that this depends on the age of the mice (Mansfield et al. 2009).

The neuropathogenic potential between TBEV strains and mutants can be compared by different experimental parameters that include time from the beginning of first symptoms to death after infection (intracranially or peripherally) and determination of the 50% lethal dose (LD_{50}) as well as determination of 50% infectious dose (ID_{50}) (Christian W. Mandl 2005). In order to determine these latter parameters, LD_{50} as parameter of neuroinvasiveness and ID_{50} as parameter of seroconversion (the time period during which specific antibody develops and becomes detectable in the blood) in the surviving mice, different inoculating doses were given to mice. Strains that have high LD_{50} and low ID_{50} (expressed as LD_{50}:ID_{50} ratio or "attenuation index") are most desirable for descriptions of strain attenuation (Kofler et al. 2003).

1.1.4 The replication cycle and mechanisms that affect TBEV neuropathogenesis

As noted at the beginning, TBEV belongs to genus *Flavivirus*. Flaviviruses are small, enveloped RNA viruses that encode three different structural proteins: glycoprotein E (envelope), protein C (capsid) and protein M (membrane that is formed by cleavage from its precursor prM) and also seven non-structural proteins: NS1 (glycoprotein), NS2A, NS2B (protease component), NS3 (protease, helicase and NTPase activity), NS4A, NS4B, NS5 (RNA-dependent polymerase) (Vilibić-Čavlek et al. 2014). Flaviviral genome is a single-stranded RNA of positive polarity that carries a 5'-cap structure (important for stability and translation of mRNA) but not 3'-polyadenylate tail (Christian W. Mandl 2005). Figure 3 depicts representation of TBEV virus virion structure.

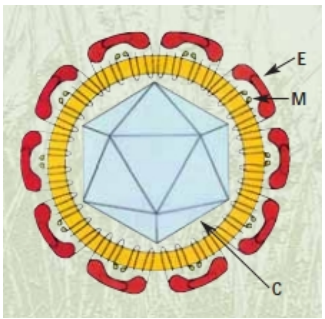

Figure 3: Schematic representation of TBEV virus: Virus capsid (C) that contains viral RNA and protein C is surrounded by assembly of the viral envelope containing protein M membrane (M) and glycoprotein E (E). (Tick-Borne Encephalitis (TBE, FSME) Monograph 2007).

Viral envelope protein E, together with the major host cell receptor, heparan sulfate (HS), serves as a mediator in binding virions to the surface of the host cell. HS is a large polysaccharide molecule with a high negative charge. It is exceedingly present in many types of cells. Different viral families, not only flaviviruses or TBEV, attach *via* this molecule. It seems that viral affinity for HS plays an important role in determining the neuroinvasiveness of TBEV (Kroschewski et al. 2003; C W Mandl et al. 2001).

Research of the *West Nile Virus* (WNV) showed that virions' transport to prelysosomal endocytic compartments of the host cell occurs by receptor-mediated endocytosis *via* clathrin-coated pits (J. J. H. Chu and Ng 2004). Between domains I and III of the E protein, protonation of the conserved histidine residue is caused by low pH in the endosome (Fritz, Stiasny, and Heinz 2008). This induces change in the conformation of the E protein that reorganizes from dimers into trimers (Allison et al. 1995). This then affects the fusion peptide that gets exposed and induces fusion of the viral membrane with the endosomal membrane. The fusion process releases the viral nucleocapsid into the cytoplasm of the host cell where uncoating of the viral RNA genome occurs (Franz X Heinz and Allison 2003). The genomic RNA serves directly as mRNA, which is translated to a single polyprotein. Single proteins are produced *via* proteolytic processing of the polyprotein (host and viral proteases). This initiates genome replication. Full-length negative strands genome copies serve as templates for constructing new positive RNAs strands (P. W. Chu and Westaway 1985). During the polyprotein synthesis, translocation of the surface proteins prM and E into the lumen of the endoplasmic reticulum (ER) occurs and their amino - termini are freed *via* proteolytic cleavage by host cell signalase (Nowak et al. 1989). Protein C packages the RNA genome into nucleocapsids on the cytoplasmic side of the ER membrane. Simultaneously, assembly of the viral envelope occurs by budding of the nucleocapsid into the ER lumen (Chambers et al. 1990). Nevertheless, if nucleocapsid is absent, proteins prM and E can independently form capsidless subviral particles (SVPs). These particles share pertinent functional and structural properties with infectious particles (presence of lipid membrane, a highly ordered arrangement of protein E and the main functionalities required for attachment and entry) (Ferlenghi et al. 2001; Schalich et al. 1996). Mentioned assembly produces non-infectious immature virions. They contain proteins prM and E on the viral surface in a heterodimeric association (Elshuber et al. 2003). Transportation of immature particles takes

place through the host secretory pathway. In the acidic vesicles of the late trans-Golgi network, virus maturation is accomplished *via* cleavage of prM protein by the host cell protease furin (Stadler et al. 1997). The final cleavage of prM protein into M and reorganization of protein E to fusion-competent homodimers enable fusion of transport vesicles with the plasma membrane of the host cell and subsequent liberation of the infectious mature virions (Wengler and Wengler 1989). If viral genome RNA is introduced into susceptible cells, it would produce virus progeny because it is itself infectious. (C W Mandl et al. 1997).

Protein E is important for the attachment of the virus to the host cell and its second transmembrane region has a role in virion formation (Orlinger et al. 2006). During the duplication process, it has a role in the fusion of the viral envelope with the cell membrane. This elongated molecule is aligned parallel to the surface of the virion. Even though we noted how protein E has an important role in the TBEV attachment to the host cell, it is important to emphasize how that process is rather complex and likely involves more than a single type of host cell receptor. Existence of a neuron-specific TBEV receptor is doubtful. Nevertheless, it seems how domain III of E protein serves as a receptor binding area (Rey et al. 1995). Mutations that occur in this area can most likely modulate neuropathogenesis. The main reason for this is that many of them reduce neurovirulence and neuroinvasiveness of TBEV (C W Mandl et al. 2000).

TBEV has both, 5' and 3' non-coding regions (NCRs) with conserved secondary structures. Both NCRs were proven to be involved in replication (Markoff 2003), translation and also involved in the neuropathogenesis (C W Mandl et al., 1998a; Christian W. Mandl et al., 1998b).

Protein C can also be involved in neuropathogenesis of this virus. Mutations that happen in the capsid protein cause the physical stability of infectious viral particles and also reduction of their production. The consequence of this is impaired ability of the virus to spread from its peripheral entry site, although its entry functions and replicative ability are probably completely conserved (Christian W. Mandl 2004). Furthermore, viral surface protein production is aimed toward the formation of non-infectious SVPs that do not contribute to the viral spread in the host organism but they stimulate the immune system (Christian W. Mandl 2005).

1.2 Innate and acquired immunity - an overview

Vertebrates' immune system is under a constant threat of the invasion of different pathogens including viruses, bacteria, protozoa, fungi and other microorganisms. Threats posed by environmental pathogens and foreign antigens to the organism's survival demanded the development of immune system defenses. The mammalian evolution has depended on this defense system which is comprised of innate and adapted (acquired) immunity (Husband 2002).

Physical barriers that serve to prevent infection, cell-intristic responses and innate immune responses are features of all multicellular organisms and provide prompt defence against invading pathogens. Innate immunity, also known as nonspecific immunity, is mediated by phagocytes, neutrophils and dendritic cells (DC) and responds to pathogens in a generic way providing immediate defence. In vertebrates, innate immunity recruits specific adaptive immunity. Innate immunity represents the first line of host protective activity and is evolutionary older mechanism than adaptive immunity (Alberts 2008).

Adaptive immune system consists of millions of lymphocyte clones and develops by clonal selection. Clonal selection theory proposes the selective mechanism by which from a vast number of lymphocytes of different antigen receptor specificity only those that encounter an antigen of their specificity proliferate and differentiate into effector cells that help eliminate the pathogen (Charles A Janeway et al. 2001). On binding the antigen, the cell divides and produces many identical progeny or clones (Charles A Janeway et al. 2001). However, binding of the antigen alone is not enough for the differentiation to occur but a variety of signals (membrane-bound co-stimulatory signals and secreted signals originating from cytokines) provided by specialized cells is required.These signals are provided by dendritic cells (DCs) for T cells, which then provide further signals for B cells. Effector B cells then secrete antibodies which can act over long distances, unlike effector T cells that act locally (they can kill infected host cells). Regulatory T cells serve to regulate lymphocytes that react against self molecules. Specific for the adaptive immunity is the proliferation and differentiation of B cells and T cells into memory cells. When the same pathogen attacks again, immune response is faster, owing to the presence of these memory cells. Both, B cells and T cells continuously circulate *via* the blood and lymph. They proliferate and differentiate (into either effector or memory cells) only when they encounter their specific foreign antigen (Alberts 2008).

Microorganisms that invade a vertebrate host are initially recognized by the innate immune system through germline-encoded pattern-recognition receptors (PRRs). These are proteins expressed by the cells of the innate immune system which recognize specific microbial components, known as pathogen-associated molecular patterns (PAMPs), which are common to microbes but not to mammals. PAMPs are essential for the survival of microorganisms and hence difficult to alter (Akira, Uematsu, and Takeuchi 2006). PRRs also recognize damage-associated molecular patterns (DAMPs) which are molecules released by host's cells during the cell damage or death (Alberts 2008).

1.3 Innate immune defenses

There are three lines of innate immune defenses: 1) physical and chemical barriers including skin, stomach acid, mucus, the normal flora, 2) innate defenses such as phagocytic digestion or degradation of double-stranded RNA intermediate in viral replication and 3) specialized proteins and phagocytic cells able to recognize pathogens due to their common conserved domains. Innate immune system is required to activate acquired immune responses *via* extracellular signaling (Alberts 2008).

When microorganisms break through physical barriers of the host defence, the innate (and adaptive) immune system must be able to distinguish these non-self molecules from self-ones in order to destroy them. Innate immune system achieves this by the recognition of specific components present in invading pathogens that are simultaneously absent in host, i.e. they are pathogen-associated. These molecules are called "pathogen-associated or microbe-associated immunostimulants" and they trigger inflammatory responses or/and phagocytosis. Examples of these immunostimulants include: formylmethionine-containing peptides as bacterial translation initiator (eukaryotic methionine is not formylated), peptidoglycan cell wall and flagella of bacteria, mannan, glucan and chitin in the cell walls of fungi, short bacterial/viral DNA sequences or even concentration-based differences of immunostimulants that are also present in normal flora. Because they often appear in repeating pattern, they are referred to as "pathogen-associated molecular patterns" (PAMPs) and are recognised by pattern recognition receptors (PRRs) (as mentioned earlier) (Alberts 2008).

PRRs are divided into several families: 1) Toll-Like Receptors (TLRs), 2) C-type Lectin Receptors, 3) Nod-Like Receptors (NLR), 4) RIG-Like receptors (RLRs) and 5) AIM-Like Receptors (ALR). The first two families belong to the transmembrane proteins found in the

plasma membrane, whereas the latter three are proteins located in intracellular compartment (Jang et al. 2015). Proteins related to TLRs and NODs are apparently involved in innate immunity in all multicellular organisms (Alberts 2008)**.** TLR family will be focused on in more details on the following pages, on as it is related to this research work. Furthermore, viral recognition by TLRs and especially TLR-independent viral recognition followed by induction of interferons production is emphasized due to the research topic.

1.3.1 Toll-Like Receptors (TLRs)

TLRs are evolutionarily conserved type I transmembrane glycoproteins whose large extracellular domain contains a series of leucine-rich-repeats (LRRs) of varying number and a cytoplasmic signaling domain homologous to that of the interleukin 1 receptor (IL-1R), termed the Toll/IL-1R homology (TIR) domain (Akira, Uematsu, and Takeuchi 2006). LRR domains are composed of 19-25 tandem LRR motifs, each of which is 24-29 amino acids in length, containing the motif XLXXLXLXX as well as other conserved amino acid residues. Each LRR consists of a β strand and an α helix connected by loops (Figure 4; Akira et al., 2006).

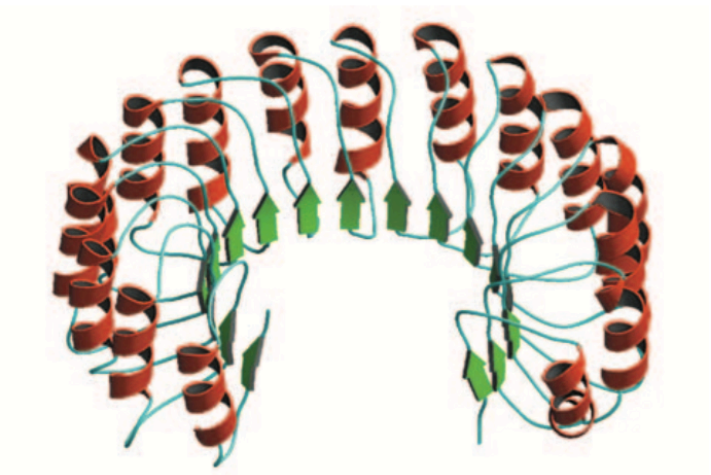

Figure 4: The three-dimensional structure of leucine-rich-repeats. LRR domains are composed of 19-25 tandem LRR motifs; each LRR consists of a β strand and an α helix connected by loops (Alberts 2008).

LRR domains have a common horseshoe structure and structure of human TLR3 LRR motifs suggests that negatively charged dsRNA binds the outside convex surface, though it remains unclear how general this model is for other TLR family members. 12 members of TLR family have been characterized in mammals until now (in mice), 10 of which are present in humans (TLR1 to TLR10). They may be expressed extracellularly on the cell surface (TLRs

1, 2, 4, 5, and 6) or intracellularly in endosomal- or lysosomal-compartments and the endoplasmic reticulum (TLRs 3, 7, 8 and 9) (Figure 5; (Yamamoto and Takeda 2010). TLR10 homolog in mice is found to be a pseudogene due to retroviral insertion (Yamamoto and Takeda 2010). TLRs can be divided into several subfamilies based on the recognition of related PAMPs: the subfamily that recognizes lipids (TLRs 1, 2 and 6), the subfamily that recognizes nucleic acids (TLRs 7, 8, 9 – believed to have evolved from one another; Boehme & Compton, 2004) and the subfamily whose members can recognize several structurally unrelated ligands (TLR4). TLRs are expressed on both, immune (macrophages, dendritic cells and some others) and non-immune cells (epithelial cells and fibroblasts) and their expression is modulated in response to pathogens, cytokines and environmental stress.

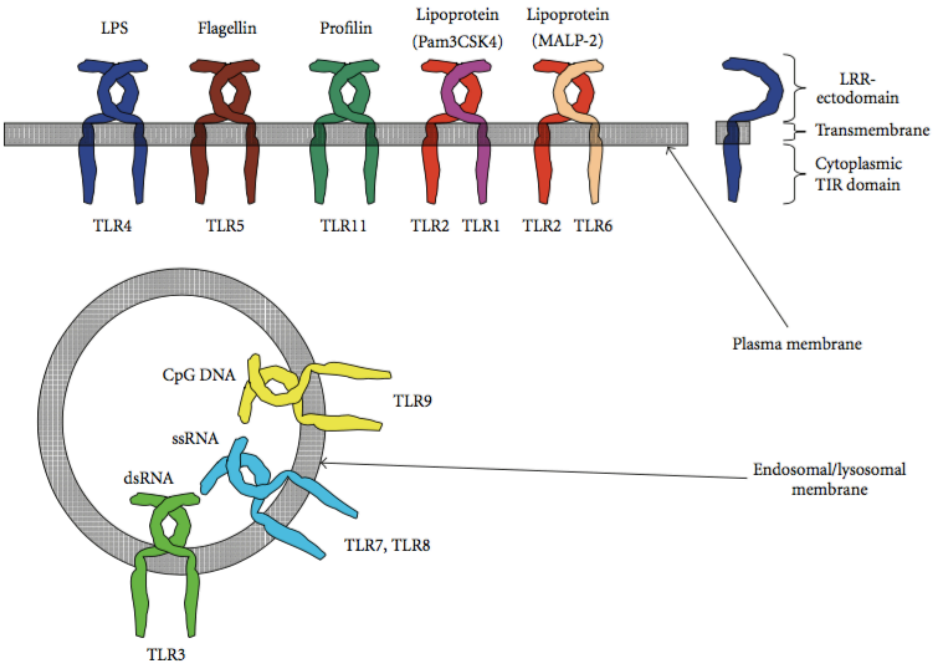

Figure 5: Localization of different TLRs. Extracellularly on the cell surface (TLRs 1, 2, 4, 5, 6 and 11) or intracellularly in endosomal/lysosomal membrane (TLRs 3, 7, 8 and 9) (Yamamoto and Takeda 2010).

TLRs signaling pathway activation originates from cytoplasmic TIR domain and activates the same signaling molecules used in IL-1R signaling (Akira, Uematsu, and Takeuchi 2006). Upon cell stimulation with TLR ligands, TIR domains of TLRs differentially recruit TIR domain-containing signaling adaptor proteins such as myeloid differentiation factor 88 (MyD88), translocating chain-associating membrane (TRAM) protein, TIR-domain-containing adapter protein (TIRAP) and TIR-domain-containing adapter protein inducing interferon-β (TRIF) (Kawasaki and Kawai 2014). Depending on the

nature of the adaptor used, different signaling pathways are triggered leading to the induction of pro-inflammatory cytokines and chemokines and Type I or Type III interferons (IFNs) or IFN-inducible genes (Figure 6; “Toll-Like Receptor Signaling Pathways: R&D Systems,” n.d.).

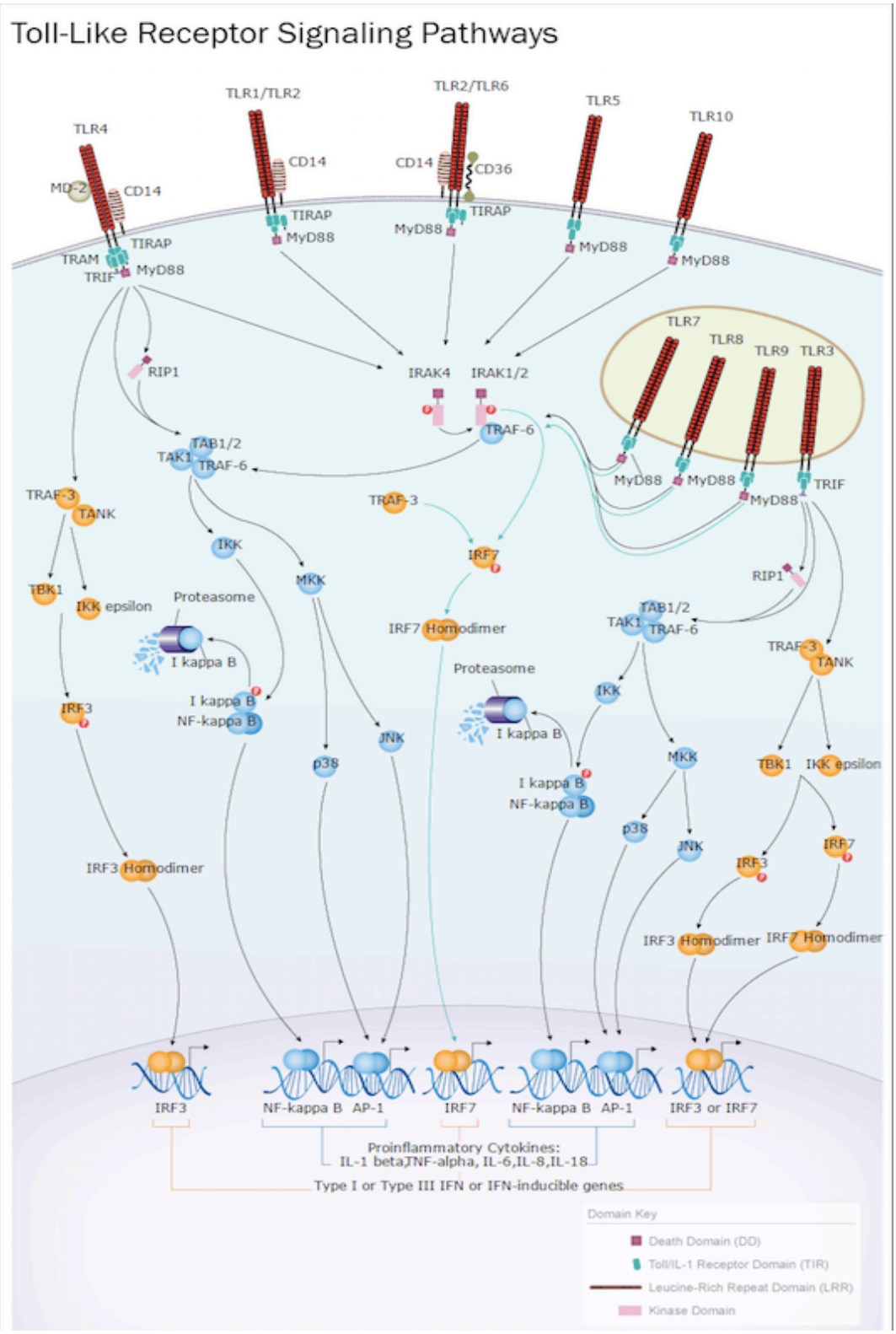

Figure 6: Toll-like receptor signaling pathways. Depending on the nature of the adaptor used, different signaling pathways are triggered leading to induction of pro-inflammatory cytokines and chemokines and Type I or Type III interferons of IFN-inducible genes (Review on Toll-Like Receptors (TLR) and TLR pathways - Invivogen n.d.).

1.3.2 Viral recognition by TLRs

Viruses have either DNA or RNA but not both composing their genetic material. Nucleic acid may be single-stranded DNA (ssDNA), double-stranded DNA (dsDNA), double-stranded RNA (dsRNA) or single stranded (ssRNA). TLRs 3, 7, 8 and 9 recognize viral nucleotides upon which they activate type I IFN production (Akira, Uematsu, and Takeuchi 2006).

DNA viruses such as herpes simplex virus 1 and 2 (HSV-1 and HSV-2) are recognized by TLR9. TLR9 is activated in response to genomes rich in unmethylated CpG DNA motifs that are more prevalent in microbial than mammalian DNA and activate inflammatory cytokines and type I IFN secretion (Akira, Uematsu, and Takeuchi 2006; LAMPHIER et al. 2006). The TLR9-mediated IFN-α response to HSV-1 and HSV-2 is cell type specific and limited to plasmacytoid dendritic cells (pDCs), a DC subpopulation characterized by their ability to secrete high levels of IFN in response to viral infection (Akira, Uematsu, and Takeuchi 2006).

ssRNA have been found to be the PAMP for TLR7 and TLR8. They are activated by specific guanine nucleotide analogs and imidazoquinolines. They employ similar mechanism of reaction to that of TLR9 to recognize distinct nucleic acid targets and react to them. The key factor for distinction between viral and self RNA seems to be the expression of TLR7 and TLR8 in endosomal membrane. Self RNA becomes degraded by extracellular RNases, whereas sheltered enveloped viruses are taken up by phagolysosomes that damage viral particles thus releasing ssRNA for TLR7 or TLR8 recognition (Akira, Uematsu, and Takeuchi 2006; Boehme and Compton 2004).

Viral dsRNA and synthetic analog of dsRNA, polyinosine-deoxycytidylic acid (poly I:C), are recognized by TLR3 localized on endosomal membrane which induces type I IFN responses. dsRNA is generated as a replication intermediate for ssRNA viruses. It is hypothesized that dsRNA that can be detected by TLR3 is released during lysis of virus-infected cells (Boehme and Compton 2004). TLR3 is expressed specifically in conventional dendritic cells (cDCs) and restricted to intracellular compartments but not in pDCs but also in astrocytes and glioblastoma brain cell lines. It's role in antiviral response is not yet

completely clear as it was earlier believed to play the key role since dsRNA is universal viral PAMP. However, it has been shown that it is not required for initial, cell-autonomous recognition (Akira, Uematsu, and Takeuchi 2006).

TLR2 and TLR4 recognize viral-envelope glycoproteins and in response activate production of inflammatory cytokines rather than type I IFNs. Glycoproteins play role in virus' binding and/or entry. Contact between TLR2 and TLR4 with the viral envelope on the cell surface thus detects pathogens even before gene expression is activated (Boehme and Compton 2004).

1.3.3 TLR-independent viral detection mechanism of RNA helicases and dsRNA *via* RIG-I

TLR3 which recognizes dsRNA is localized in endosomal membrane and thus unable to recognize dsRNA synthesized in the cytoplasm or that originating from viral genome already released in the cell. However, it seems that TLR system is not required for type I IFNs induction in most cell types. RIG-I has been identified as a cytoplasmic dsRNA detector.

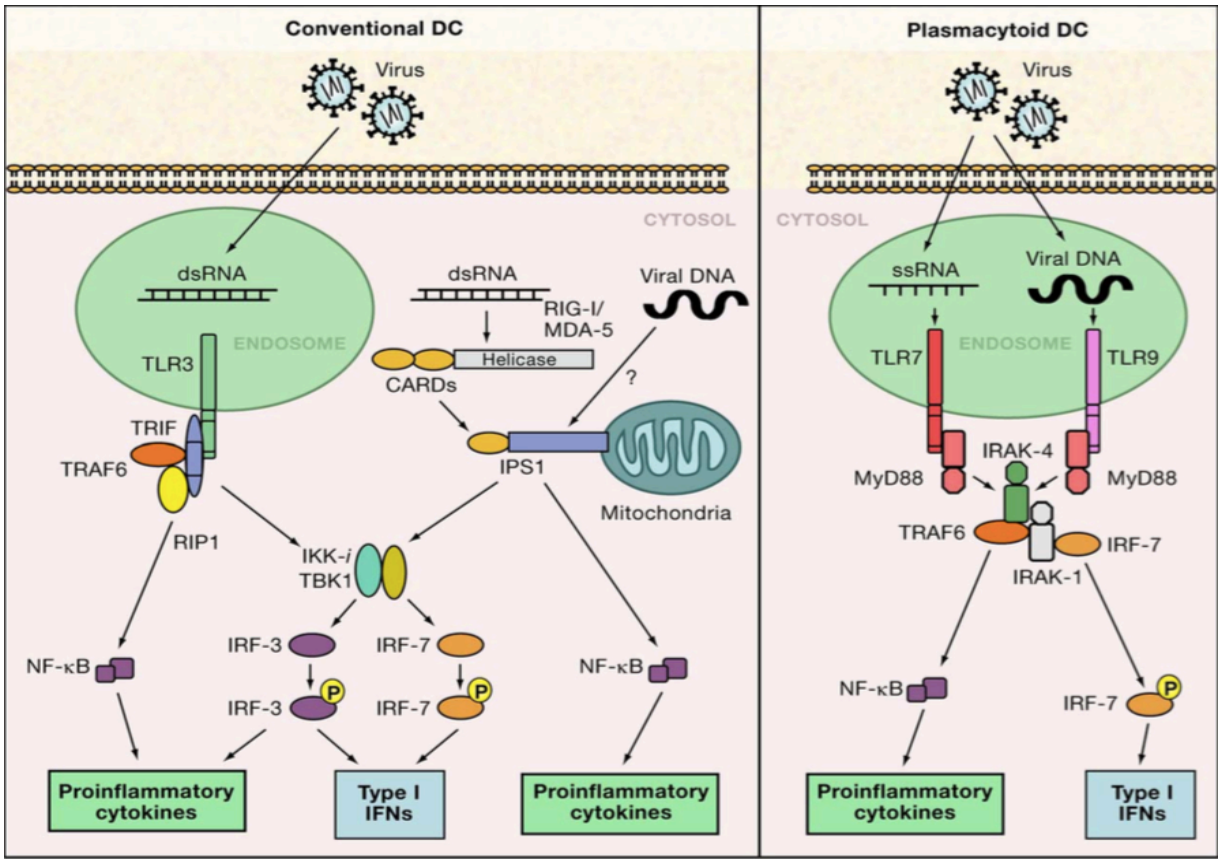

Figure 7: Viral detection mechanisms and innate immune response (Akira, Uematsu, and Takeuchi 2006).

Retinoic-acid-inducible protein I (RIG-I) is involved in innate immune response as a cytoplasmic sensor of viral RNA in response to which it induces type I IFNs (alpha and beta) and proinflammatory cytokines (Figure 7; Akira et al., 2006). It is essential for the type I IFN responses induction upon RNA virus infection (Akira, Uematsu, and Takeuchi 2006). RIG-I can detect both, positive and negative strand RNA viruses and recognizes ssRNA as well as dsRNA (including dsRNA produced from non-self dsDNA by RNA polymerase III). It contains DExD/H-box RNA helicase domain (C-terminal) and an N-terminal caspase recruitment domain (CARD).

Another homologous gene to RIG-I – melanoma differentiation associated gene 5 (MDA5) – has also been identified in viral dsRNA. Both receptors were shown to bind poly I:C. IFN-β promoter stimulator 1 (IPS-1) has been identified as an adaptor for RIG-I and MDA5 that is identified *via* their CARD domains (IPS-1 possesses resembling N-terminal CARD domain) (Akira, Uematsu, and Takeuchi 2006).

Difference between TLR3 and RIG-I viral dsRNA recognition is dependent on their localization (endosomal membrane and cytoplasm, respectively) irrespective of their route of entry. Although most cells produce type I IFN response in TLR3-independent way, TLR3 system is prevalent in pDCs (Akira, Uematsu, and Takeuchi 2006).

1.3.4 IFN-inducible OAS and RNaseL antiviral response

Oligoadenylate synthetases (OAS) are members of IFN-stimulated genes (ISGs). OAS are characterized by their ability to synthesize 2',5'- phosphodiester-linked oligoadenylates. These molecules with uncommon 2',5'- phosphodiester bond induce RNA degradation by activating the latent form of RNase L. Degraded RNA activates RIG-I and MDA5 leading to IFN induction and thus establishes an antiviral RNA decay pathway. OAS act as PRRs for detection of viral dsRNA in cytosol as they are naturally expressed in cells at low levels (as other ISGs, they are not expressed in naïve cells) (Malathi et al. 2007).

There are four OAS genes identified in humans: OAS1, OAS2, OAS3 and OASL (OAS-like) together representing at least 7 alternatively spliced genes (Guo et al. 2012). They show homology to each other encoding one (OAS1), two (OAS2) and three (OAS3) OAS domains. OAS domain exists in OASL as well but as dysfunctional due to mutations at key residues. Each form is expressed and induced differentially and each functional form has unique biological function. Recent findings suggest that OAS may play further function in antiviral response independently of RNaseL (Sun et al. 2013).

1.3.5 Human OAS-Like (OASL) protein and its isoforms

Since OASL possesses N-terminal OAS domain (Figure 8; Zhu et al., 2015), despite lacking its synthetase activity, OASL belongs to OAS family of proteins and it is believed to be derived from OAS1 (Zhu, Ghosh, and Sarkar 2015). OASL is unique in OAS family in that it possesses two ubiquitin-like domains (UBL) located in the C-terminus that are not found in other OAS family members. UBL domain is considered to play a role in OASL antiviral response.

OASL gene is comprised of 6 exons (Figure 9; Guo et al., 2012). So far, four OASL isoforms have been identified in humans, designated OASL a, OASL b, OASL c and OASL d, where OASL a, b and d are identified as having antiviral activity (Guo et al. 2012).

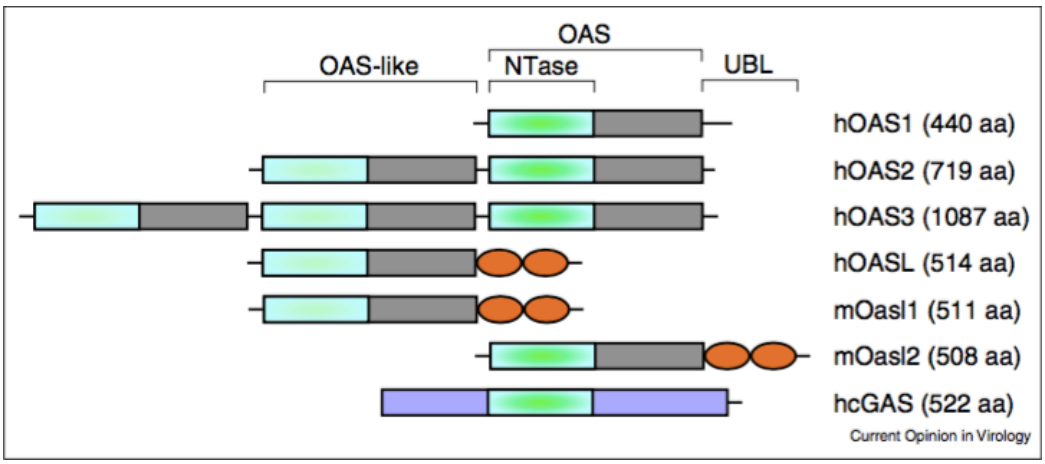

Figure 8: Domains of human OAS family and mouse OASL proteins. Human OASL proteins possess the OAS domain, but they lack their synthetase activity (Zhu, Ghosh, and Sarkar 2015).

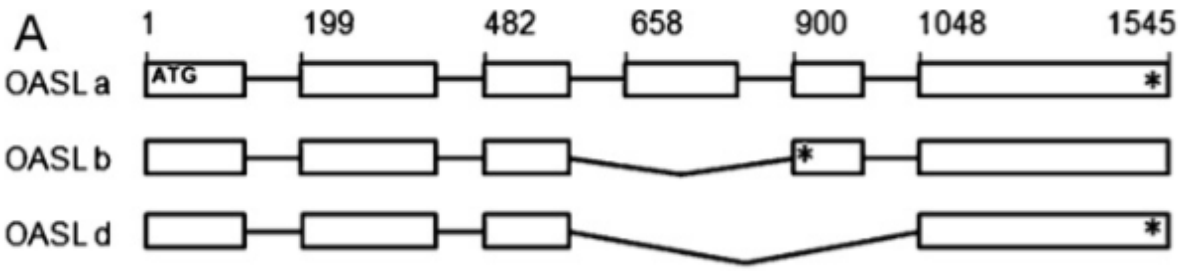

Figure 9: Gene structures of OASL isoforms. The OASL (OASL a –wild type) gene consists of 6 exons; OASL d has exons 4 and 5 deletion and OASL b lacks exon 4 which leads to the frameshift and creation of new stop codon in the beginning of exon 6 (Guo et al. 2012).

OASL a (wild-type) isoform consists of all 6 exons, whereas OASL b lacks exon 4 which leads to the frameshift and creation of new stop codon in the beginning of exon 6.

OASL d variant lacks exons 4 and 5, however, the reading frame is intact. OASL a, OASL b and OASL d are detected as approximately 59, 30 and 45 kDa proteins, respectively. All three isoforms possess identical N-terminus (exons 1, 2 and 3) that consists of 219 amino acid residues. OASL a and OASL d also share C-terminus sequence. Ubiquitin-like homology domains are comprised in C-terminal exon 6 and OASL b lacks the ubiquitin-like domain. The sequence of OASL b exon 5 differs from that of OASL an exon 5 (Guo et al. 2012).

1.3.6 Antiviral activity of human OASL protein

Human OASL proteins are shown to exhibit antiviral activity against RNA viruses (Marques et al., 2008; Rebouillat et al., 1998). Zhu et al. (2014) showed that when compared to Oasl1 (mouse orthologue of human OASL gene) human OASL indicated unique antiviral function. Mouse Oasl1 was found to enhance viral replication by strongly binding to 5' UTR of mouse IRF7 (binding was less strongly to the 5' UTR of human IRF7) whereas binding of the human OASL to either of IRF7s was not detected to inhibit its translation (Zhu et al. 2014). Furthermore, stable expression of human OASL in various cell lines indicated antiviral activity against a range of viruses (reduced virus replication but also reduced antiviral activity in the absence of RIG-I (Zhu et al. 2014)). Zhu et al (2014) in the same study showed that the expression of OASL enhances sensitivity of RIG-I signaling whereas loss of OASL expression reduces ISG induction and enhances virus replication (Ishibashi, Wakita, and Esumi 2010; Marques et al. 2008; Zhu et al. 2014).

The mechanism of OASL enhancement of RIG-I signaling is proposed to be *via* mimicking polyubiquitin. Proposed mode of RIG-I activation is as follows (Zhu, Ghosh, and Sarkar 2015): Upon viral RNA binding to RIG-I through the C-terminal domain where helicase domain is located, the helicase changes its conformation so as to enable RIG-I to hydrolyze ATP and further interact with RNA. This is followed by RIG-I activation *via* K-63 linked polyubiquitination of N-terminal CARDs by ubiquitin ligases TRIM25 and Riplet, followed by CARD domain interaction with mitochondrial protein MAVS. This interaction results in formation of MAVS aggregates and signaling that induces type I interferons. In the case of long ($\leq$ 112 bp) RNA binding, RIG-I oligomerization can occur without polyubiquitin (pUb) by ATP-dependant oligomerization whereas pUb is required for short dsRNA (<60 bp) and RNA-independent oligomerization. Both pUb and RNA binding is in most cases required for RIG-I activation. However, in the presence of OASL, OASL UBL

(ubiquitin-like) domain interacts with RIG-I by mimicking K63 linked pUb (Zhu et al. 2014).

To summarize, OASL expression is induced in human cells (human embryonic kidney cells used in the cited research) upon viral infection with single - stranded RNA viruses (Marques et al. 2008; Schoggins et al. 2011). OASL subsequently binds RIG-I by mimicking K63 linked pUb as one of the ligands required for it activation what now makes complete RIG-I activation more sensitive. Viral RNA is the second RIG-I ligand and upon successful RIG-I activation, IFNs induction is enhanced. Hence, OASL expression makes RIG-I system to become activated more sensitive to viral RNA detection rather than inducing IFN response by itself.

2. Goals

Human OASL proteins are shown to exhibit antiviral activity against RNA viruses (Marques et al., 2008; Rebouillat et al., 1998). The protein has three different isoforms (OASL a, b and d) identified as having antiviral activity (Guo et al. 2012). Zhu et al. (2014) reported that antiviral activity of human OASL protein is mediated by enhancing signaling of the RIG-I sensor. Our lab has previously described an upregulation of OASL and RIG-I genes in TBEV-infected DAOY (Selinger et al. 2017). The main goal of the bachelor thesis will be to determine the expression of all three isoforms in different time points of the infection in human brain cell lines (glioblastoma, medulloblastoma and neuroblastoma) on the mRNA level (qPCR).

3. Materials and methods

3.1 Cells and culture media

DAOY (DAOY HTB-186) and SK-N-SH (HTB-11) were purchased from ATCC and grown in low-glucose DMEM medium supplemented with 10% foetal bovine serum (FBS), 1% antibiotic/antimycotic (amphotericin B 0.25 μg $m1^{-1}$, penicillin G 100 units/ml and streptomycin 100 μg ml^{-1}) and 1% L-glutamine. U373 MG Uppsala were kindly provided by T. Eckschlager (Charles University in Prague) and grown in IMDM medium supplemented with 10% FBS, 1% antibiotic/-antimycotic (amphotericin B 0.25 μg ml^{-1}, penicillin G 100 units/ml, and streptomycin 100 μg ml^{-1}) and 1% L-glutamine.

The DAOY medulloblastoma cell line was derived from desmoplastic cerebellar medulloblastoma and the SK-N-SH neuroblastoma was derived from neuroblastoma (brain; derived from metastatic site: bone marrow). U373 MG Uppsala glioblastoma cell line was derived from malignant glioma/astrocytoma.

3.2 Subculturing of adherent cells

Cell lines were obtained from the assistant supervisor in T25 25 cm^2 flasks in cca. 10 mL of meia for sub-culturing. Adherent cells were sub-cultured for several days in 1:2 or 1:5 splitting ratios (incubation at 37°C and 5% CO_2 atmosphere). The procedure was carried out under the sterile conditions (biosafety box). Before the start, cultures were controlled under

the inverted light microscope to confirm bacterial/fungal contaminants absence and degree of confluency (cca. 80%). Spent media was removed and cell monolayer was washed with equivalent amount of PBS. Cells were next trypsinized with 0,5 mL of 0,25% trypsin in HBSS and the flask was rotated so as to cover the entire monolayer and left for several minutes for cells to detach. Cell detachment was examined under the inverted light microscope and a small amount of medium was added to inactivate trypsin. An equal amount (to initial) of fresh media (pre-warmed) was added to the flask and the required volume (taking into account the split ratio) was transferred into new flask and the flask was topped to required volume.

3.3 Cell seeding

The procedure as described above for sub-cultivation up until cell detachment was carried out. After cell detachment 100 μL of re-suspended cells were added to 100 μL trypane blue (1:1 mixing ratio) and counted using Bürker chamber and light microscope. 25 squares were counted for three times to calculate an average cell count. Cell concentration [cells/mL] was calculated as follows: average count * 2 * 10 000 (multiplication by 2 due to the dilution ratio and by 10 000 due to correction factor to reach counting chamber volume to be 1 mL). The flask with cell suspension was stored in the fridge to prevent cell attachment.

Dilution ratios for seeding were calculated to obtain required number of cells per well (Tables 1 and 2). Higher number of neuroblastoma cells was used as compared to glioblastoma and medulloblastoma as it was found that when using lower number of neuroblastoma cells, cells were dying. Cells were let to attach for 24 hours incubated at 37°C and 5% CO_2 atmosphere.

Samples from Table 1 were seeded in 24-well plates and were used for the purpose of RT-PCR. Samples from Table 2 were seeded in 6-well plates and were used for the purpose of qRT-PCR. Different number of glioblastoma and medulloblastoma cells per well shown in Table 2 is due to lesser volume of media added (22,10 mL instead of 24,10 mL). All samples were prepared in biological triplicates.

Table 1: Detailed cell seeding information used for RT-PCR.

							Mixing Ratio				
Cell line	Count 1	Count 2	Count 3	Average Count	Concentration [cells/mL]	Total Volume of cell suspension [mL]	Cells [mL]	Medium [mL]	Final conc. [cells/mL]	Volume/Well [mL]	Cells/Well
U373	189	188	188	188	3766667,00	25,00	1,00	24,00	150000,00	0,80	120000
DAOY	105	68	84	86	1713333,00	25,00	2,20	22,80	150000,00	0,80	120000
SK-N-SH	129	112	114	118	2366667,00	20,00	1,70	18,30	200000,00	0,80	160000

Table 2: Detailed cell seeding information used for qRT-PCR.

							Mixing Ratio				
Cell line	Count 1	Count 2	Count 3	Average Count	Concentration [cells/mL]	Total Volume of cell suspension [mL]	Cells [mL]	Medium [mL]	Final conc. [cells/mL]	Volume/Well [mL]	Cells/Well
U373	168	176	161	168	3366667,00	24,00	1,90	22,10	267000,00	2,00	534000
DAOY	62	46	46	51	1026667,00	26,00	6,10	19,92	240000,00	2,00	480000
SK-N-SH	154	149	128	144	2873333,00	26,00	5,10	20,93	560000,00	2,00	1120000

3.4 TBEV infection

All the work with TBEV was performed under BSL2 conditions. The low-passage TBEV strain Neudoerfl (fourth passage in suckling mice brains; GenBank accession no. U27495) was provided by Professor F. X. Heinz (Medical University of Vienna, Austria) (F. X. Heinz and Kunz 1981) All cell lines were infected at a multiplicity of infection (MOI) of 5. In case of 24-well/6-well plates 0,2/1,0 mL of viral suspension per well were added, respectively. Mock suspensions were prepared analogically to the viral ones.

Medium from wells was discarded and required volumes of brain suspensions were added to wells. The virus was let to attach to the cells for 2 hours. After attachment, suspensions were discarded and cells were washed with sterile PBS (volume the same or greater than the volume of viral / mock suspension) and fresh medium was added. Cells were incubated at 37°C and 5% CO_2 atmosphere.

3.5 Cell harvesting and RNA isolation

Cells were washed with sterile PBS. 50 μL (24-well plates) or 100 μL (6-well plates) of trypsine was added to each sample and left for cca 5 minutes for cells to detach. Next, 0,3 mL of fresh medium was added per sample and cells were re-suspended. Cell suspension was transferred to a 1,5-mL microtube and centrifuged for 5 min at 500 x *g*. The medium was discarded and PBS was added, cells were re-suspended and spinned for 5 min at 500 x *g*. PBS was then discarded and cells frozen in liquid nitrogen and stored at -80°C in the case of samples from 24-well plates. In the case of samples from 6-well plates 350 μL of lysis buffer RA1 from NucleoSpin® RNA II kit (Macherey-Nagel) was added and stored at -80°C. Cells were collected in designed time intervals: 24, 48 and 72 hours post infection (hpi).

Total RNA was isolated using NucleoSpin® RNA II kit (Macherey-Nagel) as described in the manufacturer's protocol. Cells were lysed in 350 μL of lysis buffer RA1 (Buffer RA1 and ß-mercaptoethanol in 100:1 ratio, respectively) and lysates were filtrated. 350 μL ethanol was added to flowthrough and mixed by pipetting up and down 5 times. Lysates were loaded to the NucleoSpin® RNA II Column placed in a Collection Tube and centrifuged for 30s at 11000 x *g*. Column was placed in a new collection tube, 350 μL of Membrane Desalting Buffer was added and centrifuged for 1 min at 11000 x *g*. Onto the center of dry silica membrane 95 μL of DNase (reconstitutuent rDNase and Reaction Buffer

for rDNase in 1:9 ratio respectively) reaction mixture was applied and membrane was incubated for 15 minutes. Afterwards, the silica membrane was washed three times: the first wash with 200 μL Buffer RA2 (centrifuge for 30s at 11000 x *g*) and the second and the third wash with 600 μL and 250 μL, respectively, with Buffer RA3 (centrifuge for 30s at 11000 x *g* after the second wash and 2 min at 11000 x *g* after the third wash.) RNA used in RT-PCR was eluted in 25 μL of RNase-free H_2O, whereas RNA used in RT-qPCR was eluted in 40 μL of RNase-free H_2O and centrifuged for 1 min at 11000 x *g*.

Concentration of RNA in samples was determined using nanophotometer (Table 3; Implen P-300, Germany).

3.6 RT-PCR (reverse transcription-polymerase chain reaction)

In order to digest genomic DNA (gDNA) contaminations in RNA isolates, 300 ng of total RNA from each sample was first treated with dsDNase (Thermo Scientific). Reactions were prepared according to the scheme in Table 3.

Table 3: Concentration and purity of RNA isolates with volumes used for dsDNase treatment.

Cell line	hpi	Infection	RNA concentration [ng/μL]	A260/A280	A260/A230	Volume of RNA needed for 0,3 μg in reaction [μL]	Volume of water to 10 μL [μL]
U373	24	Mock	129,00	2,013	2,013	2,3	7,7
			54,40	2,030	1,545	5,5	4,5
			80,40	2,010	0,966	3,7	6,3
		TBEV	51,60	1,985	0,921	5,8	4,2
			58,00	1,986	0,954	5,2	4,8
			60,00	2,027	0,279	5,0	5,0
	48	Mock	232,00	2,046	1,856	1,3	8,7
			156,00	2,026	1,995	1,9	8,1
			168,00	2,034	1,091	1,8	8,2
		TBEV	68,40	2,036	1,745	4,4	5,6
			54,00	2,077	0,241	5,6	4,4
			76,00	2,088	0,160	3,9	6,1
	72	Mock	209,00	2,019	2,143	1,4	8,6
			209,00	2,015	1,746	1,4	8,6
			242,00	2,034	2,090	1,2	8,8
		TBEV	61,20	2,013	1,101	4,9	5,1
			83,20	2,019	0,450	3,6	6,4
			74,00	2,056	1,581	4,1	5,9
DAOY	24	Mock	58,00	2,014	1,768	5,2	4,8
			64,40	1,988	1,288	4,7	5,3
			54,00	1,985	1,184	5,6	4,4
		TBEV	104,00	2,023	1,036	2,9	7,1
			56,00	1,972	1,111	5,4	4,6
			94,80	1,992	1,009	3,2	6,8
	48	Mock	40,40	2,020	1,656	7,4	2,6
			94,80	2,079	0,252	3,2	6,8
			68,00	2,048	0,205	4,4	5,6
		TBEV	105,00	2,047	0,478	2,9	7,1
			87,20	2,000	1,627	3,4	6,6
			106,00	2,047	0,438	2,8	7,2
	72	Mock	122,00	2,013	1,515	2,5	7,5
			88,80	2,037	1,521	3,4	6,6
			123,00	2,026	2,110	2,4	7,6
		TBEV	86,40	2,000	1,029	3,5	6,5
			139,00	2,047	1,706	2,2	7,8
			202,00	2,032	1,833	1,5	8,5
SK-N-SH	48	Mock	35,60	2,119	0,659	8,4	1,6
			39,60	2,063	1,065	7,6	2,4
			21,20	2,120	0,688	14,2	-4,2
		TBEV	41,20	2,102	0,380	7,3	2,7
			28,40	2,088	0,538	10,6	-0,6
			31,20	2,053	0,804	9,6	0,4

300 ng of RNA per sample plus RNase-free water up to 9,6 μL (exceptions: SK-N-SH cells - 48 hours post infection: mock-infected replicate no. 3 and TBEV-infected replicate no. 2; 9,6 μL of RNA was added but total amount of RNA was less than 300 ng; see Table 3, highlighted data) was added to the RNase-free reaction tube. 1,2 μL of dsDNase Buffer and 1,2 μL of dsDNase was added to it (Thermo Scientific dsDNase kit). DNase treatment was carried out for 1 hour at 37°C.

Following DNase treatment, one-step RT-PCR was performed using Platinum® Quantitative RT-PCR ThermoScript kit (Invitrogen). Reactions were prepared according to the following scheme (universal OASL primers used) and protocol (Table 4 and Table 5):

Table 4: RT-PCR reaction scheme.

ThermoScriptTM Plus RT / Platinum® *Taq* Enzyme Mix	0,5 μL
2X ThermoScriptTM Reaction Mix	12,5 μL
OASL uni F primer (10 uM)	0,75 μL
OASL uni R primer (10 uM)	0,75 μL
RNase-free H2O	3,5 μL
dsDNase-treated RNA	12,0 μL

Table 5: RT-PCR protocol.

Cycling Step	Temperature (°C)	Duration	Number of cycles
cDNA synthesis	50	30 min	1
Initial denaturation and enzyme activation	95	5 min	1
Denaturing	95	30 sec	30
Annealing	58	30 sec	
Extension	72	1 min	

Electrophoretic separation was performed on 1.5% agarose gel. For band visualization, SYBR Green was used (added in loading buffer directly to samples). GeneRuler™ 100bp Plus DNA ladder was used.

3.7 qRT-PCR (quantitative reverse transcription-polymerase chain reaction)

KAPA SYBR® FAST Universal One-Step qRT-PCR Kit (Kapa Biosystems) was used.

4,00 μL of DNase-treated RNA (18.33 ng/μL for U373 and DAOY; 19,33 ng/μL for SK-N-SH; exceptions due to insufficient RNA amount are highlighted in the Table 6) was used per reaction. Reactions were prepared according to the following scheme (Table 6 and Table 7):

Table 6: Concentration and purity of RNA isolates with volumes used for dsDNase treatment.

Cell line	hpi	Infection	RNA conce-ntration [ng/μL]	A260/ A280	A260/ A230	Volume of RNA needed for 0,3 ug in reaction [μL]	Volume of water to 10 uL [μL]	Total volume of DNase reaction [μL]	Dilution after DNase treatment [n times]	Final RNA conce-ntration [ng/μL]
U373	24	Mock	226,00	2,112	0,682	9,7	2,3	15,0	8,0	18,33
			348,00	2,069	2,251	6,3	5,7	15,0	8,0	18,33
			313,00	2,061	2,244	7,0	5,0	15,0	8,0	18,33
		TBEV	363,00	2,059	2,220	6,1	5,9	15,0	8,0	18,33
			333,00	2,059	1,921	6,6	5,4	15,0	8,0	18,33
			245,00	2,047	2,242	9,0	3,0	15,0	8,0	18,33
	48	Mock	290,00	2,074	2,187	7,6	4,4	15,0	8,0	18,33
			455,00	2,058	2,205	4,8	7,2	15,0	8,0	18,33
			263,00	2,066	2,212	8,4	3,6	15,0	8,0	18,33
		TBEV	322,00	2,067	2,161	6,8	5,2	15,0	8,0	18,33
			499,00	2,056	2,182	4,4	7,6	15,0	8,0	18,33
			530,00	2,037	2,192	4,2	7,8	15,0	8,0	18,33
DAOY	24	Mock	182,00	2,078	0,983	12,1	-0,1	15,0	8,0	18,33
			290,00	2,069	2,123	7,6	4,4	15,0	8,0	18,33
			824,00	2,070	2,395	2,7	9,3	15,0	8,0	18,33
		TBEV	448,00	2,053	2,238	4,9	7,1	15,0	8,0	18,33
			401,00	2,064	2,204	5,5	6,5	15,0	8,0	18,33
			36,00	2,070	1,935	61,1	-49,1	15,0	8,0	3,60
	48	Mock	338,00	2,019	2,215	6,5	5,5	15,0	8,0	18,33
			276,00	2,009	2,208	8,0	4,0	15,0	8,0	18,33
			231,00	2,017	2,053	9,5	2,5	15,0	8,0	18,33
		TBEV	188,00	2,013	2,075	11,7	0,3	15,0	8,0	18,33
			221,00	2,018	2,111	10,0	2,0	15,0	8,0	18,33
			233,00	2,014	2,172	9,4	2,6	15,0	8,0	18,33
SK-N-SH	48	Mock	236,00	2,017	2,222	9,3	2,7	20,0	5,8	19,13
			290,00	2,014	2,204	7,6	4,4	20,0	5,8	19,13
			224,00	2,014	2,205	9,8	2,2	20,0	5,8	19,13
		TBEV	131,00	2,012	2,158	16,8	-4,8	20,0	5,8	13,67
			142,00	2,034	2,058	15,5	-3,5	20,0	5,8	14,82
			160,00	2,005	2,204	13,8	-1,8	20,0	5,8	16,70

Table 7: RT-qPCR reaction scheme.

PCR-grade water	2,30 μL
2x KAPA SYBR FAST qPCR Master Mix	7,50 μL
primer F 10 uM	0,45 μL
primer R 10 uM	0,45 μL
50x KAPA RT Mix	0,30 μL
Template RNA (18,33 ng/ul)	4,00 μL

Specific primers for each OASL transcript variant were used as well as primers for RIG-I and HPRT. All primers were used in the final concentration of 0,30 μM.

For RT- negative control (reaction without 50x KAPA RT Mix), 2,00 μL of DNase-treated RNA (18,33 ng/μL) was used per reaction. Total volume per reaction used was 10,00 μL with the same primer concentrations. Cycling protocol was as listed in Table 8.

Table 8: RT-PCR protocol.

Cycling Step	Temperature (°C)	Duration	Number of cycles
Reverse transcription	42	10 min	1
Enzyme inactivation	95	5 min	1
Denaturation	95	5 sec	40
Annealing/extension/ data acquisition	60	30 sec[3]	

Quantification was performed on LightCycler 480 (Roche). All data were analysed using the relative quantification (ΔΔ-Ct method) and HPRT as the reference gene.

3.8 List of used primers

All primers for OASL detection were designed by the assistant supervisor. Primers for RIG-I and HPRT qPCR detection were taken from (Teng et al. 2012) and (Vandesompele et al. 2002) respectively. Universal OASL primers (OASL uni F and OASL uni R) were designed to produce fragments with different length in order to distinguish particular OASL transcripts (Figure 10; blue arrows). Specific primers for each OASL transcript were designed in order to amplify the unique sequence of the particular transcript (Figure 10; red arrows). For sequences, see Table 9.

Table 9: Sequences of primers used.

Primer name	Sequence (5' -> 3')	Product length
OASLa-F	CCAGCAGTATGTGAAAGCCA	122 bp
OASLa-R	CGTCCAACATGAAATTCTCGTC	
OASLb-F	CAGCAGGCCCATCATCCTG	120 bp
OASLb-R	CTGTTGTCATAGCAACAGTC	
OASLd-F	GTACCAGCAGAGGGCACGAG	160 bp
OASLd-R	GGAACCTGGAAGGACAGACGC	
OASL uni F	CCTGAGGTCTATGTGAGCCTG	OASL a 561 bp OASL b 319 bp OASL d 171 bp
OASL uni R	TGTCAAGTGGATGTCTCGTGC	
RIG-I F	GCTCCTCCAGTGTCTTCTCAG	132 bp
RIG-I R	TGACAAAGTGCTCACAGTTCC	
HPRT F	TGACACTGGCAAAACAATGCA	94 bp
HPRT R	GGTCCTTTTCACCAGCAAGCT	

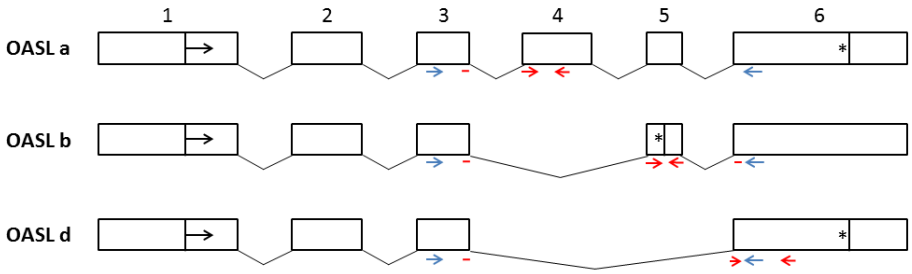

Figure 10: Schematic overview of primer design in OASL transcription variants (exons with 5' and 3' NCRs are shown). Black arrows represent ATG start codon, asterisks STOP codon. Blue arrows represent localization of OASL uni F and R primers. Red arrows represent localization of OASL a, b, d-specific primers.

4. Results

4.1 Expression of OASL transcript variants in human neural cell lines upon TBEV infection

OASL expression was shown to be induced upon TBEV infection in DAOY cells (Selinger et al., 2017). Therefore, we decided to characterize this phenomenon in more detail using also other human neural cell lines. First, we employed basic RT-PCR method to describe the presence of mRNA for OASL a, OASL b, and OASL d isoforms in three human neural cell lines of different origin – glial cells (U373) and neuronal cells (DAOY and SK-N-SH). All cell lines were infected with TBEV strain Neudoerfl (5 MOI) and the presence of OASL transcript variants was determined using one-step RT-PCR employing OASL universal primers (see chapter 3.8.). For RT-PCR analysis, total RNA isolated at 24, 48, and 72 hours post infection (hpi) was used (analysis was performed in biological triplicates).

Figure 11 depicts electrophoretic separation of OASL isoforms in TBEV- and mock-infected U373 cells at different time intervals (24, 48, and 72 hpi). Both, OASLa (561 bp) and OASL b (319 bp) isoforms were detected at all time intervals tested regardless on the presence of the TBEV. OASL a, unlike OASL b, possesses the ubiquitin-like (UBL) domain and its expression at all time intervals of infection is not as surprising as that of OASL b, which lacks the UBL domain. Interestingly, OASL d (171 bp) isoform, known for its antiviral response *via* ubiquitin-coding domain (Guo et al. 2012), was only expressed at 24 hpi in both, mock- and TBEV-infected U373 cells.

Figure 12 depicts electrophoretic separation of OASL isoforms in TBEV- and mock-infected DAOY cells at different time intervals (24, 48, and 72 hpi). As in the case of U373 cells, OASL a (561bp) and OASL b (319 bp) isoforms were both detected at all time intervals tested, regardless on the presence of TBEV. OASL d isoform was not detected in DAOY cells.

Due to the insufficient amount of RNA isolated from SK-N-SH cells at 24 and 72 hpi, only 48 hhpi time interval was used for RT-PCR analysis. No OASL mRNA for any of the isoforms was detected (Figure 13).

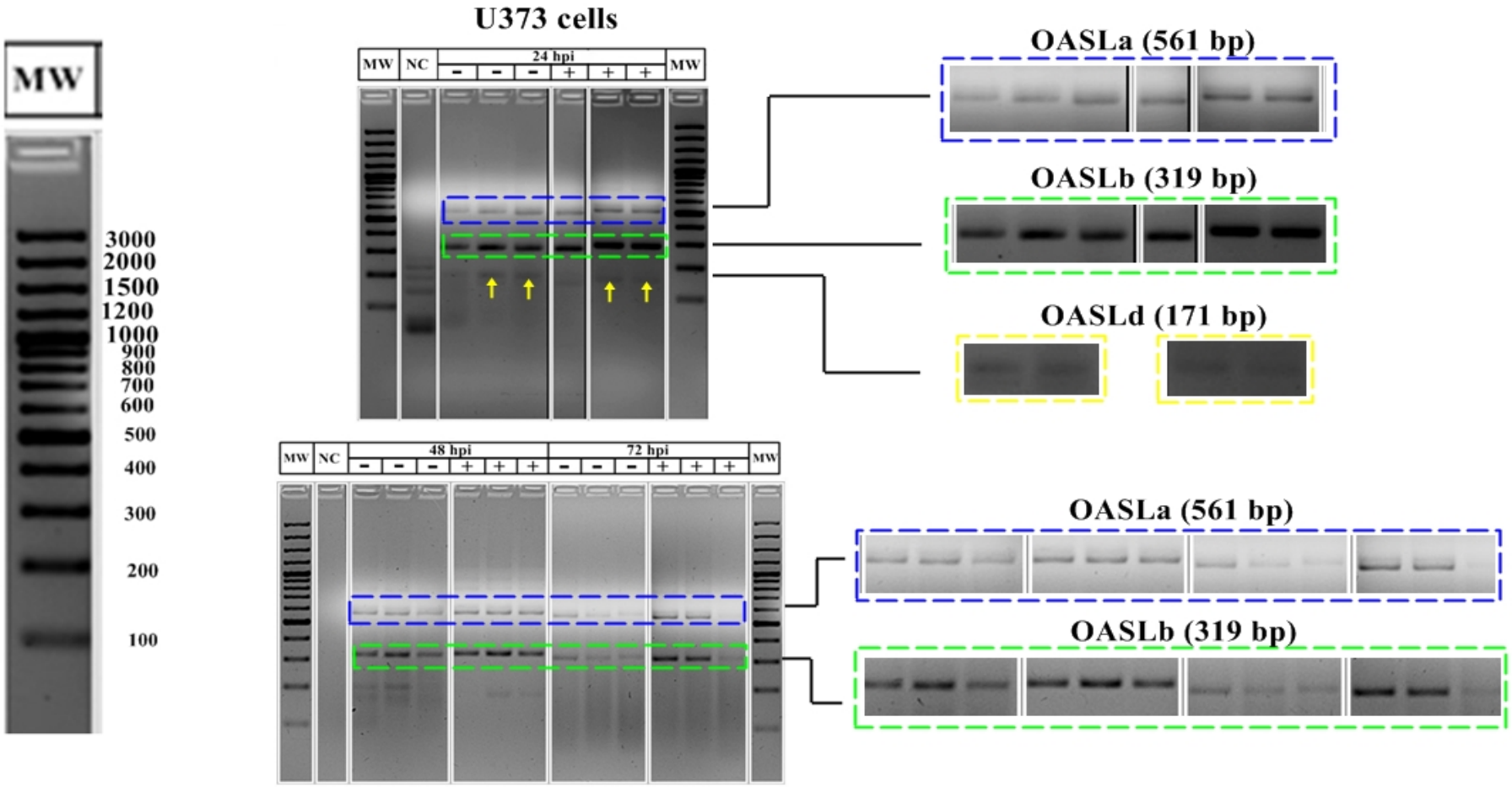

Figure 11: Electrophoretic separation of RT-PCR products (OASL a = 561 bp; OASL b = 319 bp; OASL d = 171 bp) in mock-infected (-) and TBEV-infected (+) U373 cells at different time intervals of infection (24-72 hpi); MW = molecular weight marker (GeneRuler™ 100bp Plus DNA ladder); NC = no template control.

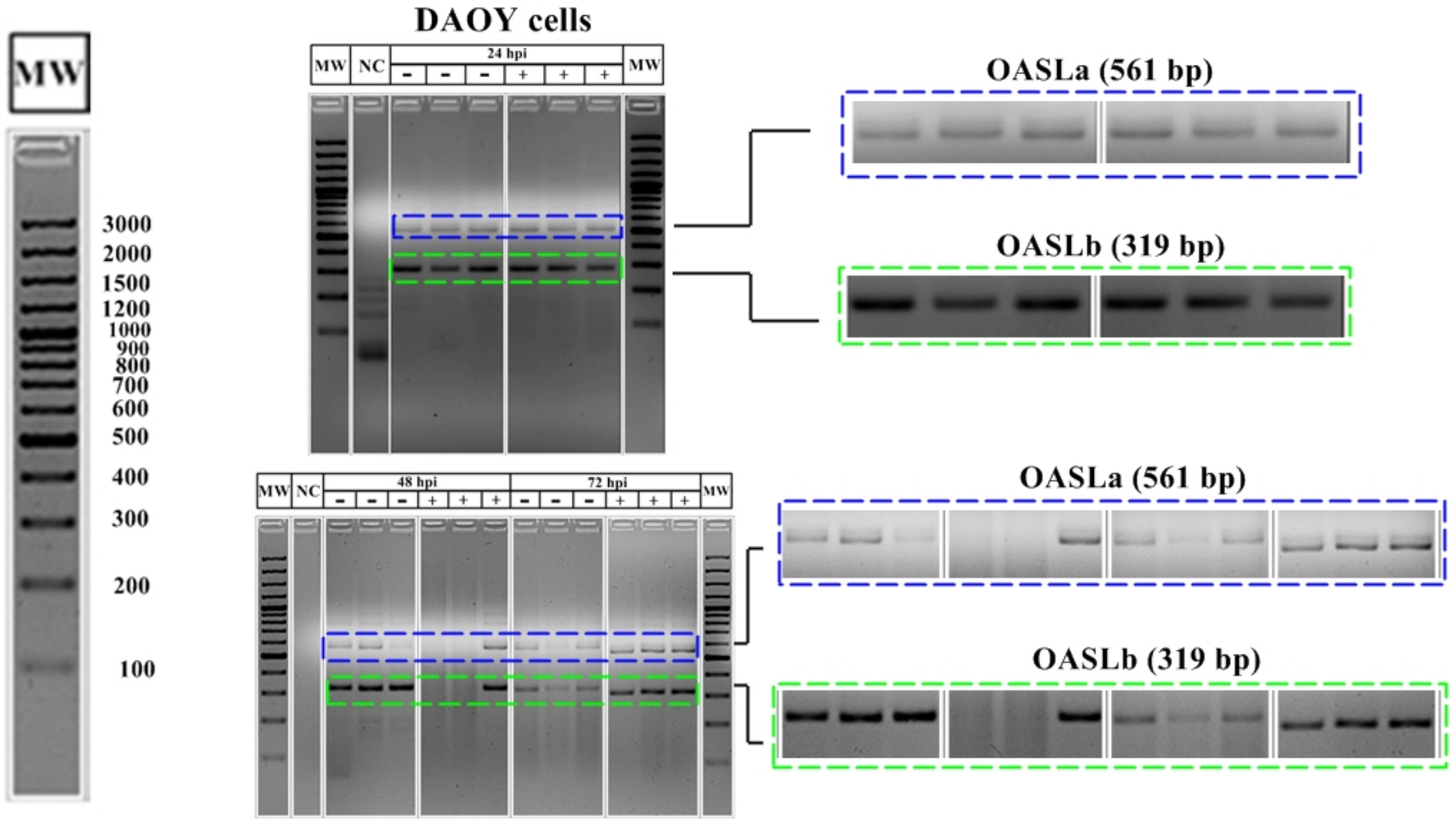

Figure 12: Electrophoretic separation of RT-PCR products (OASL a = 561 bp; OASL b = 319 bp; OASL d = 171 bp) in mock-infected (-) and TBEV-infected (+) DAOY cells at different time intervals of infection (24-72 hpi); MW = molecular weight marker (GeneRuler™ 100bp Plus DNA ladder); NC = no template control.

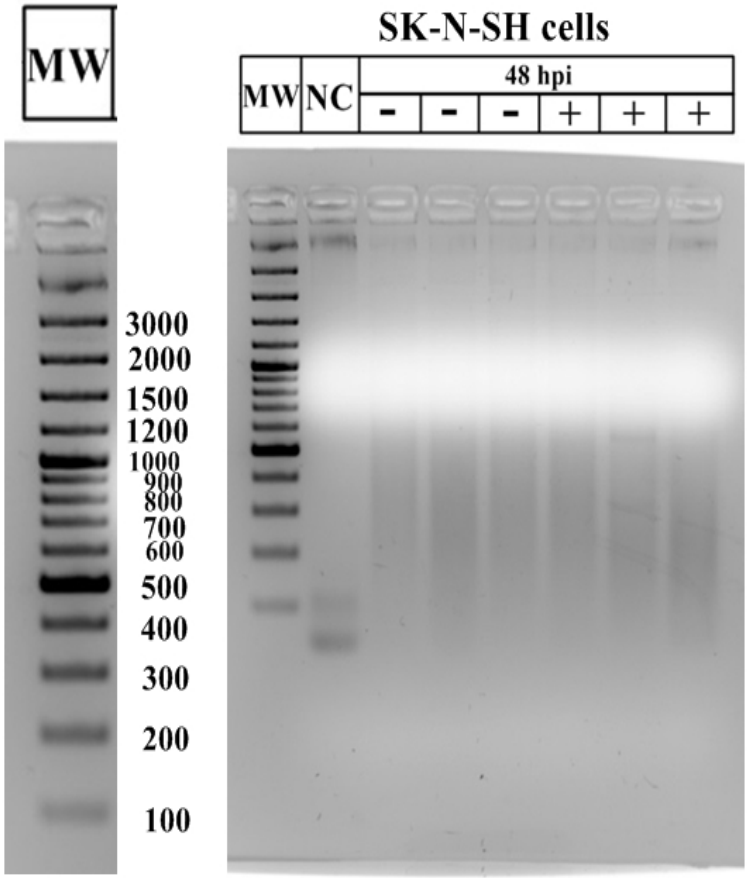

Figure 13: Electrophoretic separation of OASL isoforms in mock-infected (-) and TBEV infected (+) SK-N-SH cells at 48 hours after infection (hpi = hours post infection) – none of the isoform products (OASL a = 561 bp; OASL b = 319 bp; OASL d = 171 bp) was detected; MW = molecular weight marker (GeneRuler™ 100bp Plus DNA ladder); NC = no template control.

4.2 Relative quantification of OASL and RIG -I expression in human neural cell lines upon TBEV infection

Since RT-PCR is only a qualitative method, we decided to quantify the up-regulation of OASL expression using qRT-PCR. Three sets of primers were used in order to quantify each OASL transcription variant (see chapters 3.7. and 3.8.). New set of samples was prepared (all in biological triplicates): U373, DAOY and SK-N-SH cells were infected with TBEV Neudoerfl strain and total RNA was isolated at 24 and 48 hpi. In addition to OASL, analysis of RIG-I expression was also performed in order to determine if OASL and RIG-I induction are related, since it was showed that human OASL protein mediated activation of RIG-I RNA-sensor signaling (Zhu et al. 2014).

Relative quantification of OASL transcription variants present in U373 cells showed that all three OASL transcription variants were more upregulated at 48 hpi rather than at 24 hpi (Figure 14 and 15). In more detail, only OASL d variant was significantly upregulated in TBEV-infected cells at 24 hpi with 5,29±1,15-fold increase (Figure 14, Table 10). Even though OASL a isoform upregulation was the highest (6,02±4,12), the difference was not statistically significant from mock-infected cells (Table 10). OASL b isoform was also not significantly upregulated; the fold-increase was in the lowest when compared to the remaining two isoforms (2,40±0,97 fold increase). All three variants were significantly upregulated at 48 hpi in U373 cells (Figure 15, Table 11), with 34,88±5,96-fold, 12,56±3,41-fold, and 8,50±2,37-fold for OASL a, OASL b, and OASL d, respectively. The induction rates show that OASL a isoform is dominantly expressed.

The general expression profile of OASL transcription variants in DAOY cell line followed similar pattern as in the case of U373 cells – all three transcription variants were documented to be highly upregulated at 48 hpi rather than at 24 hpi (Figure 14 and 15). On the other hand, OASL b and OASL d variants were expressed in higher ration to OASL a unlike in U373 cells. No statistically significant increase in mRNA levels was observed for all three variants at 24 hpi. In more detail, OASL d variant fold-increase was the highest (2,49±2,46), followed by OASL a (1,46±1,67) and OASL b (0,93±1,03). However, as shown in Figure 15 and Table 11, expression of all three isoforms was significantly induced at 48 hpi. OASL b and OASL d mRNA levels increased in a very similar way: 21,40±6,46-fold and 24,53±6,12-fold, respectively. In case of OASL a variant 34,53±3,03-fold increase was observed.

As seen in Figure 15 and Table 11, a significant increase in OASL mRNA levels was observed in SK-N-SH cells at 48 hpi. However, in comparison to the U373 and DAYO cells, documented increase was very low. Moreover, the expression pattern at 48 hpi was the same as in the case of U373 and DAOY: OASL a shows the highest fold-increase (2,26±0,40), followed by OASL d (1,88±0,11) and OASLb (1,76±0,12).

In case of RIG-I expression, U373 cells were documented to strongly upregulate its expression upon TBEV infection. Interestingly, the strong upregulation was observed already at 24 hpi (26,62±7,74-fold increase; Figure 16 and Table 12) and was even increased after next 24 hours (30,44±1,07-fold; Figure 17 and Table 13). DAOY cells, in comparison, showed no significant increase at 24 hpi (1,52±0,26; Figure 16 and Table 12). However, a significant increase in RIG-I expression was observed at 48 hpi in DAOY cells (Figure 17

and Table 13). Unlike other cell types, SK-N-SH cells did not show any significant change in RIG-I expression at 48 hours of infection (Figure 17 and Table 13).

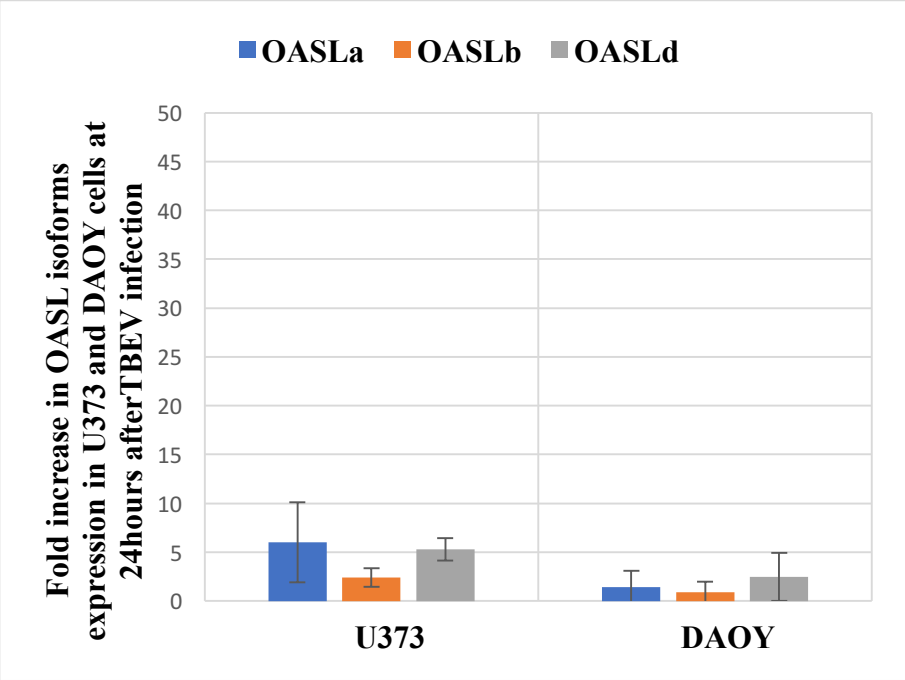

Figure 14: Fold-increase in OASL a, OASL b and OASL d expression in U373 and DAOY cells at 24 hours post TBEV infection.

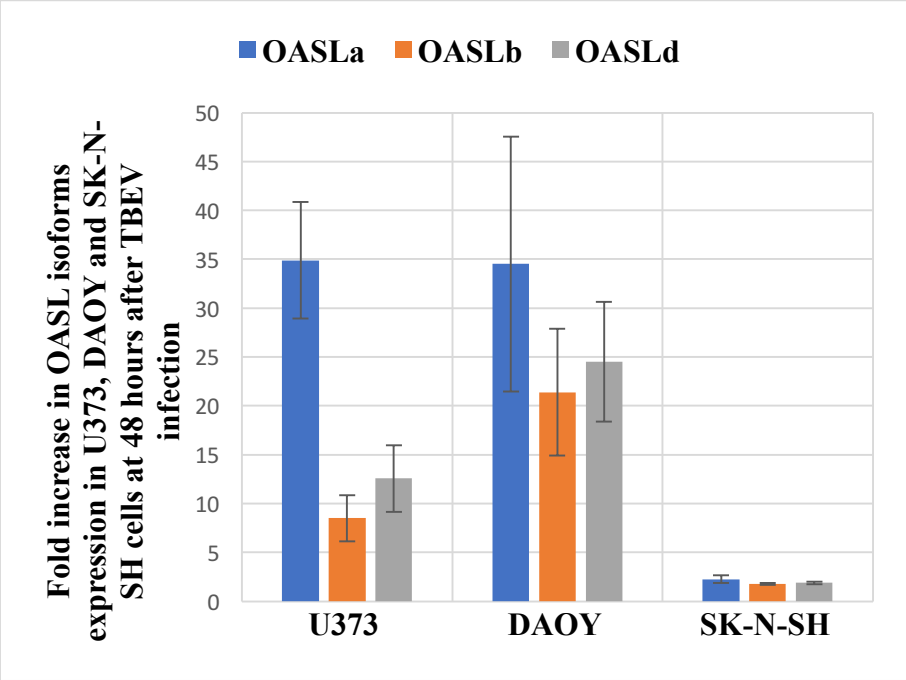

Figure 15: Fold-increase in OASL a, OASL b and OASL d expression in U373, DAOY, and SK-N-SH cells at 48 hours post TBEV infection.

Table 10: Student's t-test p-values for tested difference between mock- and TBEV-infected cells (α=0,05). Asterisk symbolizes significantly different values (p<α).

24 hpi	OASL a	OASL b	OASL d
U373	0,159658	0,111076	0,006180 *
DAOY	0,716867	0,929986	0,149854

Table 11: Student's t-test p-values for tested difference between mock- and TBEV-infected cells (α=0,05). Asterisk symbolizes significantly different values (p<α).

48 hpi	OASL a	OASL b	OASL d
U373	0,001301 *	0,010977 *	0,008704 *
DAOY	0,021997 *	0,011105 *	0,005567 *
SK-N-SH	0,011176 *	0,000739 *	0,000367 *

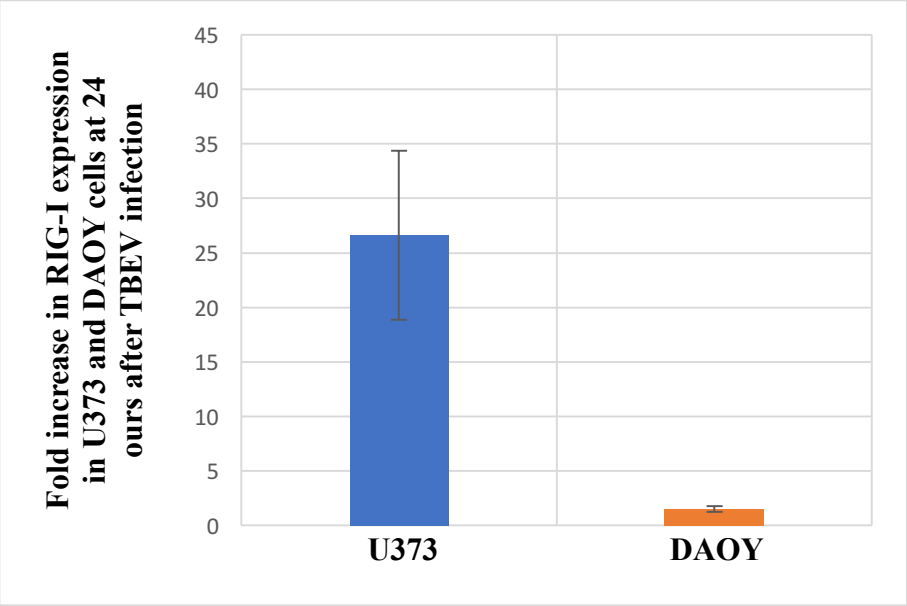

Figure 16: Fold increase in RIG-I expression in U373 and DAOY cells at 24 hours post TBEV infection.

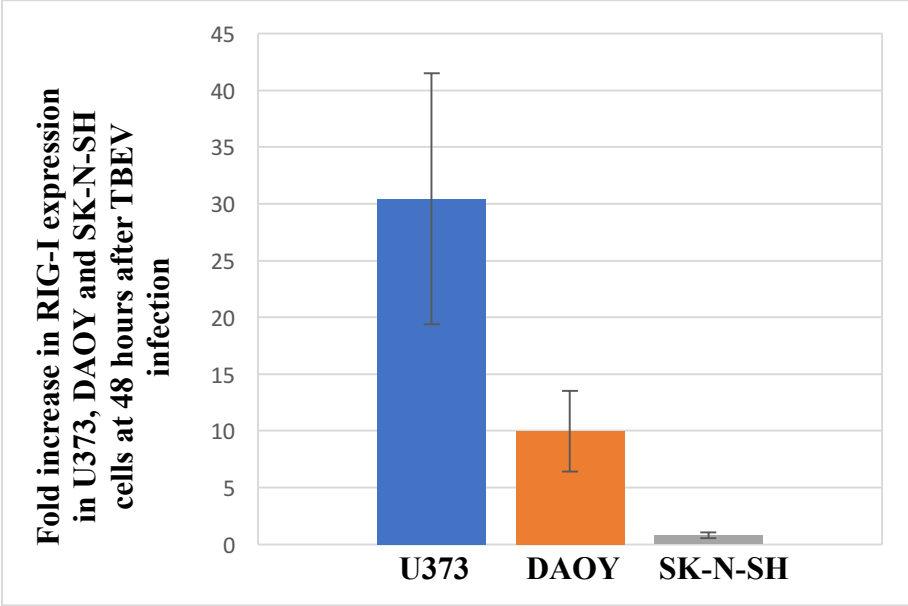

Figure 17: Fold increase RIG-I expression in U373, DAOY, and SK-N-SH cells at 48 hours post TBEV infection.

Table 12: Student's t-test p-values for tested difference between mock- and TBEV-infected cells (α=0,05). Asterisk symbolizes significantly different (p<α).

24 hpi	RIG-I
U373	0,009432 *
DAOY	0,050408

Table 13: Student's t-test p-values for tested difference between mock- and TBEV-infected cells (α=0,05). Asterisk symbolizes significantly different (p<α).

48 hpi	RIG-I
U373	0,019783 *
DAOY	0,022976 *
SK-N-SH	0,356465

5. Discussion

TBEV flavivirus is known to be highly neurotropic. Růžek et al. (2009) examined the TBEV infection in neuroblastoma, glioblastoma and medulloblastoma cell lines in order to clarify the interaction of TBEV with neural cells and showed that TBEV is lethal to all three cell lines. They reported that infection of glioblastoma and medulloblastoma cells with TBEV was associated with a number of apoptotic morphological changes. On the other hand, neuroblastoma cells exhibited necrotic morphological features and cells were dying preferentially by necrotic mechanism.

Human OASL gene has been reported to be rapidly induced byinterferon regulatory factor 3 (IRF3) and type I IFNs. For an antiviral activity of OASL against RNA viruses, the UBL domain was shown to play a major role (Marques et al. 2008; Schoggins et al. 2011; Zhu et al. 2014). Zhu et al. (2014) reported that antiviral activity of human OASL protein is mediated by enhancing signaling of the RIG-I sensor. Our lab has previously described an upregulation of OASL in TBEV-infected DAOY cells (Selinger et al. 2017), as well as significant upregulation of RIG-I gene responsible for sensing viral RNA. Therefore, we decided to characterize this phenomenon in more detail using also other human neural cell lines.

At first, we employed basic RT-PCR method to describe the expression profile of OASL transcript variants (OASLa, OASLb and OASLd) in human neural cell lines (glioblastoma – U373, medulloblastoma – DAOY, and neuroblastoma – SK-N-SH) upon TBEV infection. Next, we decided to quantify the up-regulation of OASL transcription variants using qRT-PCR.

U373 and DAOY cells exhibited constant expression of OASL a transcription variant regardless of TBEV infection, and at all inspected time intervals (24, 48 and 72 hours after infection). Moreover, qRT-PCR results show that the OASL a transcription variant was the most upregulated one in both cell lines. This is consistent with the available data, where OASL a isoform is the main variant being expressed (Choi et al. 2015a). Interestingly, the expression profile of OASL b mRNA in U373 and DAOY cells was the same as for the OASL a. OASL b lacks the ubiquitin domain, which is known to be relevant for the antiviral response of OASL protein (Choi et al. 2015b; Marques et al. 2008). Therefore, the expression of OASL b isoform at later intervals of TBEV infection (48 and 72 hours) can point to its possible antiviral role in case of TBEV. OASLd isoform, known for its antiviral response *via* ubiquitin-coding domain as in the case of OASL a (Guo et al. 2012), is the only isoform that was not detected in all three cell lines *via* RT-PCR. Only slight bands were

visible in U373 cells (both, mock- and TBEV-infected) at 24 hours hpi. qRT-PCR analysis revealed a significant induction of expression in case U373 cells at 24 hpi, culminating at 48 hpi. DAOY cells started to express OASL d at 48 hpi. The possible explanation of conflicting results between RT-PCR and qRT-PCR could be the higher sensitivity of qRT-PCR due to the usage of specific primers and higher number of cycles.

SK-N-SH cells were not found to express OASL gene in either of isoforms (RT-PCR) and a very low induction was documented using qRT-PCR. As mentioned in the theoretical part, neurons are a primary target of TBEV (Kaiser 1999) and TBEV-infected neuroblastoma cells are dying preferentially by necrotic mechanism (Růžek et al., 2009). Therefore, no or very low expression of OASL in SK-N-SH cells could be one of the factors contributing to the high sensitivity of neurons to TBEV resulting in necrosis.

Considerably strong induction of RIG-I expression in U373 cells at both, 24 and 48 hpi, indicates an important role of this receptor in response to TBEV infection. Expression of OASL isoforms at the same considered time intervals revealed relevant increase of OASLa and OASL d especially. This is in accordance with the proposed mechanism of OASL antiviral activity where OASL enhances sensitivity of RIG-I signaling *via* binding to RIG-I by mimicking K63 linked pUb as one of the ligands required for it activation (Zhu et al. 2014). Thus, the possible model upon infection of U373 cells with TBEV could be following: RIG- I senses the RNA virus (TBEV) and triggers the signaling cascade leading to IFN production. IFN stimulate the expression of OASL as well as RIG-I (positive feedback loop). Produced OASL enhances the sensitivity of RIG-I and the viral spread is reduced. Moreover, the high sensitivity and responsiveness of U373 cells in terms of OASL and RIG-I expression could be linked to their glial origin. Glial cells (astrocytes and microglia) were shown to be a major producer of type I IFN in CNS during La Crosse Virus infection in mice (Kallfass et al. 2012).

RIG-I expression in DAOY cells was significantly increase at later time interval (48 hpi) when compared to U373 cells. Possible explanation could be the absence of IFN-β production in DAOY cells upon TBEV infection (Selinger et al., 2017). However, despite no type I IFN signaling in DAOY cells, a significant induction of OASL expression was documented. This suggests an existence of an alternative signaling cascade leading to the induction of OASL expression. One of the possible factors involved in this IFN-independent induction of OASL expression could be the IRF3/IRF7 signalling cascade which was shown to induce human OASL expression (Melchjorsen et al. 2009).

Moreover, a further study describing OASL protein levels is required to investigate possible virus' targeting of OASL translation and/or protein degradation in order to oppose the antiviral function of OASL, especially with regards to RIG-I signaling. It was shown that the nonstructural proteins of RSV (respiratory syncytial virus) suppress the host cell's IFN response by targeting multiple members of the IFN induction and response pathways, such as RIG-I, IRF3, IRF7, and degradation of these substrates. Moreover, RSV NS1 protein promotes proteasome-dependent OASL degradation (Dhar et al. 2015). Similarly, inhibition of IFN-triggered signaling cascade by Zika virus (ZIKV; Wu et al., 2017) plays a critical role for ZIKV to evade antiviral responses from host cells (ZIKV sfRNA inhibits RIG-I signaling).

6. Conclusions

Glioblastoma cells showed constant expression of OASL a and OASL b isoforms and a significant increase in OASL a and OASL d isoforms in TBEV infected cells at 48 hpi. These results point out to the potential importance of OASL a and OASL d isoforms in this cell line. Strong and early induction of RIG-I expression further supports the proposed mechanism of co-dependence of RIG-I activation by OASL *via* mimicking K63 linked pUb as both OASL a and OASL d contain ubiquitin-like domains.

OASL a and OASL d expression in DAOY cells was shown to be similar to that in U373 cells with the difference being that upregulation of both isoforms was approximately the same (in U373 cells, OASL a increase was approximately twice to that of OASL b). However, an interesting finding was discovered in OASL b expression in this cell line. OASL b isoform was not only constantly expressed at different time intervals of TBEV-infected and healthy cells but its expression was also meaningfully increased at 48 hours after TBEV infection. The importance of this upregulation remains to be elucidated as OASL b isoform lacks the ubiquitin-like domain, as well as its expression on the protein level.

SK-N-SH cells showed no or very low upregulation of all OASL isoforms in response to TBEV.

7. References

Akira, Shizuo, Satoshi Uematsu, and Osamu Takeuchi. 2006. "Pathogen Recognition and Innate Immunity." *Cell* 124(4): 783–801. http://www.ncbi.nlm.nih.gov/pubmed/16497588%0Ahttp://linkinghub.elsevier.com/retrieve/pii/S0092867406001905.

Alberts, Bruce et al. 2008. *Molecular Biology of the Cell*. 5th ed. New York: Garland Science, pp. 1485 - 538

Allison, Steven L et al. 1995. "Oligomeric Rearrangement of Tick-Borne Encephalitis Virus Envelope Proteins Induced by an Acidic pH." 69(2): 695–700.

Boehme, Karl W, and Teresa Compton. 2004. "Innate Sensing of Viruses by Toll-like Receptors." *Journal of virology* 78(15): 7867–73. http://www.ncbi.nlm.nih.gov/pubmed/15254159 (August 7, 2017).

Brinton, Margo A, and Andrey A Perelygin. 2003. "Genetic Resistance to Flaviviruses." *Advances in virus research* 60: 43–85. http://www.ncbi.nlm.nih.gov/pubmed/14689691 (August 12, 2017).

Chambers, Thomas J., Chang S. Hahn, Ricardo Galler, and Charles M. Rice. 1990. "Flavivirus Genome Organization, Expression, and Replication." *Annual Review of Microbiology* 44(1): 649–88. http://www.ncbi.nlm.nih.gov/pubmed/2174669 (August 12, 2017).

Charles A Janeway, Jr, Paul Travers, Mark Walport, and Mark J Shlomchik. 2001. "Principles of Innate and Adaptive Immunity." https://www.ncbi.nlm.nih.gov/books/NBK27090/ (August 7, 2017).

Choi, Un Yung, Ji-Seon Kang, Yune Sahng Hwang, and Young-Joon Kim. 2015a. "Oligoadenylate Synthase-like (OASL) Proteins: Dual Functions and Associations with Diseases." *Experimental & molecular medicine* 47(3): e144. http://www.ncbi.nlm.nih.gov/pubmed/25744296 (August 14, 2017).

Choi, Un Yung, Ji Seon Kang, Yune Sahng Hwang, and Young Joon Kim. 2015b. "Oligoadenylate Synthase-like (OASL) Proteins: Dual Functions and Associations with Diseases." *Experimental & Molecular Medicine* 47(3): e144. http://dx.doi.org/10.1038/emm.2014.110.

Chu, J J H, and M L Ng. 2004. "Infectious Entry of West Nile Virus Occurs through a Clathrin-Mediated Endocytic Pathway." *Journal of virology* 78(19): 10543–55. http://www.ncbi.nlm.nih.gov/pubmed/15367621 (August 12, 2017).

Chu, P W, and E G Westaway. 1985. “Replication Strategy of Kunjin Virus: Evidence for Recycling Role of Replicative Form RNA as Template in Semiconservative and Asymmetric Replication.” *Virology* 140(1): 68–79. http://www.ncbi.nlm.nih.gov/pubmed/2578239 (August 12, 2017).

Dhar, J et al. 2015. “2’ -5’ -Oligoadenylate Synthetase-Like Inhibits Respiratory Syncytial Virus Replication and Is Targeted by the Viral Nonstructural Protein 1.” *J Virol* 89(19): JVI.01076-15. [Epub ahead of print]. http://www.ncbi.nlm.nih.gov/pubmed/26178980%5Cnhttp://jvi.asm.org/content/89/19/10115.full.pdf.

Elshuber, S., Steven L Allison, Franz X Heinz, and Christian W Mandl. 2003. “Cleavage of Protein prM Is Necessary for Infection of BHK-21 Cells by Tick-Borne Encephalitis Virus.” *Journal of General Virology* 84(1): 183–91. http://www.ncbi.nlm.nih.gov/pubmed/12533715 (August 13, 2017).

Ferlenghi, I et al. 2001. “Molecular Organization of a Recombinant Subviral Particle from Tick-Borne Encephalitis Virus.” *Molecular cell* 7(3): 593–602. http://www.ncbi.nlm.nih.gov/pubmed/11463384 (August 13, 2017).

Fritz, Richard, Karin Stiasny, and Franz X Heinz. 2008. “Identification of Specific Histidines as pH Sensors in Flavivirus Membrane Fusion.” *The Journal of cell biology* 183(2): 353–61. http://www.ncbi.nlm.nih.gov/pubmed/18936253 (August 12, 2017).

Gritsun, T. S., V. A. Lashkevich, and E. A. Gould. 2003. “Tick-Borne Encephalitis.” *Antiviral Research* 57(1–2): 129–46. http://linkinghub.elsevier.com/retrieve/pii/S0166354202002061 (August 6, 2017).

Guo, Xuancheng et al. 2012. “Identification of OASL D, a Splice Variant of Human OASL, with Antiviral Activity.” *International Journal of Biochemistry and Cell Biology* 44(7): 1133–38. http://dx.doi.org/10.1016/j.biocel.2012.04.001.

Heinz, F. X., and C. Kunz. 1981. “Homogeneity of the Structural Glycoprotein from European Isolates of Tick-Borne Encephalitis Virus: Comparison with Other Flaviviruses.” *Journal of General Virology* 57(2): 263–74.

Heinz, Franz X, and Steven L Allison. 2003. “Flavivirus Structure and Membrane Fusion.” *Advances in virus research* 59: 63–97. http://www.ncbi.nlm.nih.gov/pubmed/14696327 (August 12, 2017).

Husband, A. J. 2002. “Overview of the Mammalian Immune System.” In *Advances in Nutritional Research Volume 10*, Boston, MA: Springer US, 3–14. http://link.springer.com/10.1007/978-1-4615-0661-4_1 (August 7, 2017).

Ishibashi, Mariko, Takaji Wakita, and Mariko Esumi. 2010. “2???,5???-Oligoadenylate Synthetase-like Gene Highly Induced by Hepatitis C Virus Infection in Human Liver Is Inhibitory to Viral Replication in Vitro.” *Biochemical and Biophysical Research Communications* 392(3): 397–402. http://dx.doi.org/10.1016/j.bbrc.2010.01.034.

Jang, Ji Hyun et al. 2015. “An Overview of Pathogen Recognition Receptors for Innate Immunity in Dental Pulp.” *Mediators of Inflammation* 2015.

Kaiser, Reinhard. 1999. “The Clinical and Epidemiological Profile of Tick-Borne Encephalitis in Southern Germany 1994-98. A Prospective Study of 656 Patients.” *Brain* 122(11): 2067–78.

Kallfass, Carsten et al. 2012. “Visualizing Production of Beta Interferon by Astrocytes and Microglia in Brain of La Crosse Virus-Infected Mice.” *Journal of virology* 86(20): 11223–30. http://www.ncbi.nlm.nih.gov/pubmed/22875966 (August 14, 2017).

Kawasaki, Takumi, and Taro Kawai. 2014. “Toll-Like Receptor Signaling Pathways.” *Frontiers in Immunology* 5: 461. http://journal.frontiersin.org/article/10.3389/fimmu.2014.00461/abstract (August 7, 2017).

Kofler, Regina M et al. 2003. “Spontaneous Mutations Restore the Viability of Tick-Borne Encephalitis Virus Mutants with Large Deletions in Protein C Spontaneous Mutations Restore the Viability of Tick-Borne Encephalitis Virus Mutants with Large Deletions in Protein C.” 77(1): 443–51.

Kroschewski, Helga, Steven L Allison, Franz X Heinz, and Christian W Mandl. 2003. “Role of Heparan Sulfate for Attachment and Entry of Tick-Borne Encephalitis Virus.” 308: 92–100.

Labuda, M et al. 1996. “Importance of Localized Skin Infection in Tick-Borne Encephalitis Virus Transmission.” *Virology* 219(2): 357–66. http://www.sciencedirect.com/science/article/pii/S0042682296902615.

———. 1997. “Tick-Borne Encephalitis Virus Transmission between Ticks Cofeeding on Specific Immune Natural Rodent Hosts.” *Virology* 235(1): 138–43. http://www.sciencedirect.com/science/article/pii/S0042682297986220.

LAMPHIER, M. S et al. 2006. “TLR9 and the Recognition of Self and Non-Self Nucleic Acids.” *Annals of the New York Academy of Sciences* 1082(1): 31–43. http://www.ncbi.nlm.nih.gov/pubmed/17145922 (August 7, 2017).

Malathi, Krishnamurthy, Beihua Dong, Michael Gale, and Robert H. Silverman. 2007. “Small Self-RNA Generated by RNase L Amplifies Antiviral Innate Immunity.” *Nature*

448(7155): 816–19. http://www.ncbi.nlm.nih.gov/pubmed/17653195 (August 13, 2017).

Mandl, C W et al. 1997. “Infectious cDNA Clones of Tick-Borne Encephalitis Virus European Subtype Prototypic Strain Neudoerfl and High Virulence Strain Hypr.” *Journal of General Virology* 78(5): 1049–57. http://www.ncbi.nlm.nih.gov/pubmed/9152422 (August 12, 2017).

———. 1998. “Spontaneous and Engineered Deletions in the 3’ Noncoding Region of Tick-Borne Encephalitis Virus: Construction of Highly Attenuated Mutants of a Flavivirus.” *Journal of virology* 72(3): 2132–40. http://www.ncbi.nlm.nih.gov/pubmed/9499069 (August 12, 2017).

———. 2000. “Attenuation of Tick-Borne Encephalitis Virus by Structure-Based Site-Specific Mutagenesis of a Putative Flavivirus Receptor Binding Site.” *Journal of virology* 74(20): 9601–9. http://www.ncbi.nlm.nih.gov/pubmed/11000232 (August 12, 2017).

———. 2001. “Adaptation of Tick-Borne Encephalitis Virus to BHK-21 Cells Results in the Formation of Multiple Heparan Sulfate Binding Sites in the Envelope Protein and Attenuation in Vivo.” *Journal of virology* 75(12): 5627–37. http://www.ncbi.nlm.nih.gov/pubmed/11356970 (August 12, 2017).

Mandl, Christian W. et al. 1998. “In Vitro-Synthesized Infectious RNA as an Attenuated Live Vaccine in a Flavivirus Model.” *Nature Medicine* 4(12): 1438–40. http://www.ncbi.nlm.nih.gov/pubmed/9846585 (August 12, 2017).

———. 2004. “Flavivirus Immunization with Capsid-Deletion Mutants: Basics, Benefits, and Barriers.” *Viral Immunology* 17(4): 461–72. http://www.ncbi.nlm.nih.gov/pubmed/15671744 (August 12, 2017).

———. 2005. “Steps of the Tick-Borne Encephalitis Virus Replication Cycle That Affect Neuropathogenesis.” *Virus Research* 111(2 SPEC. ISS.): 161–74.

Mansfield, K. L. et al. 2009. “Tick-Borne Encephalitis Virus - A Review of an Emerging Zoonosis.” *Journal of General Virology* 90(8): 1781–94.

Markoff, Lewis. 2003. “5’- and 3’-noncoding Regions in Flavivirus RNA.” *Advances in virus research* 59: 177–228. http://www.ncbi.nlm.nih.gov/pubmed/14696330 (August 12, 2017).

Marques, Joao et al. 2008. “The p59 Oligoadenylate Synthetase-like Protein Possesses Antiviral Activity That Requires the C-Terminal Ubiquitin-like Domain.” *Journal of General Virology* 89(11): 2767–72.

Mashimo, T. et al. 2002. “A Nonsense Mutation in the Gene Encoding 2’-5’-oligoadenylate synthetase/L1 Isoform Is Associated with West Nile Virus Susceptibility in Laboratory Mice.” *Proceedings of the National Academy of Sciences* 99(17): 11311–16. http://www.ncbi.nlm.nih.gov/pubmed/12186974 (August 12, 2017).

Melchjorsen, Jesper et al. 2009. “Differential Regulation of the *OASL* and *OAS1* Genes in Response to Viral Infections.” *Journal of Interferon & Cytokine Research* 29(4): 199–208. http://www.ncbi.nlm.nih.gov/pubmed/19203244 (August 14, 2017).

Nowak, T, P M Färber, G Wengler, and G Wengler. 1989. “Analyses of the Terminal Sequences of West Nile Virus Structural Proteins and of the in Vitro Translation of These Proteins Allow the Proposal of a Complete Scheme of the Proteolytic Cleavages Involved in Their Synthesis.” *Virology* 169(2): 365–76. http://www.ncbi.nlm.nih.gov/pubmed/2705302 (August 12, 2017).

Orlinger, K. K., V. M. Hoenninger, R. M. Kofler, and C. W. Mandl. 2006. “Construction and Mutagenesis of an Artificial Bicistronic Tick-Borne Encephalitis Virus Genome Reveals an Essential Function of the Second Transmembrane Region of Protein E in Flavivirus Assembly.” *Journal of Virology* 80(24): 12197–208. http://www.ncbi.nlm.nih.gov/pubmed/17035331 (August 12, 2017).

Palus, Martin et al. 2017. “Tick-Borne Encephalitis Virus Infects Human Brain Microvascular Endothelial Cells without Compromising Blood-Brain Barrier Integrity.” *Virology* 507(March): 110–22. http://dx.doi.org/10.1016/j.virol.2017.04.012.

Perelygin, Andrey A et al. 2002. “Positional Cloning of the Murine Flavivirus Resistance Gene.” 99(14).

“Review on Toll-Like Receptors (TLR) and TLR Pathways - Invivogen.” http://www.invivogen.com/review-tlr (August 7, 2017).

Rey, Félix A. et al. 1995. “The Envelope Glycoprotein from Tick-Borne Encephalitis Virus at 2 Å Resolution.” *Nature* 375(6529): 291–98. http://www.ncbi.nlm.nih.gov/pubmed/7753193 (August 12, 2017).

Růzek, Daniel et al. 2009. “Morphological Changes in Human Neural Cells Following Tick-Borne Encephalitis Virus Infection.” *The Journal of general virology* 90(Pt 7): 1649–58.

Schalich, J et al. 1996. “Recombinant Subviral Particles from Tick-Borne Encephalitis Virus Are Fusogenic and Provide a Model System for Studying Flavivirus Envelope Glycoprotein Functions.” *Journal of virology* 70(7): 4549–57. http://www.ncbi.nlm.nih.gov/pubmed/8676481 (August 13, 2017).

Schoggins, John W. et al. 2011. “A Diverse Range of Gene Products Are Effectors of the Type I Interferon Antiviral Response.” *Nature* 472(7344): 481–85. http://www.ncbi.nlm.nih.gov/pubmed/21478870 (August 14, 2017).

Selinger, Martin et al. 2017. “Analysis of Tick-Borne Encephalitis Virus-Induced Host Responses in Human Cells of Neuronal Origin and Interferon-Mediated Protection.” *The Journal of general virology*. http://www.microbiologyresearch.org/content/journal/jgv/10.1099/jgv.0.000853.v1%0Ahttp://www.ncbi.nlm.nih.gov/pubmed/28786780.

Stadler, K, S L Allison, J Schalich, and F X Heinz. 1997. “Proteolytic Activation of Tick-Borne Encephalitis Virus by Furin.” *Journal of virology* 71(11): 8475–81. http://www.ncbi.nlm.nih.gov/pubmed/9343204 (August 13, 2017).

Sun, L. et al. 2013. “Cyclic GMP-AMP Synthase Is a Cytosolic DNA Sensor That Activates the Type I Interferon Pathway.” *Science* 339(6121): 786–91. http://www.ncbi.nlm.nih.gov/pubmed/23258413 (August 13, 2017).

Teng, Terk-Shin et al. 2012. “Viperin Restricts Chikungunya Virus Replication and Pathology.” *Journal of Clinical Investigation* 122(12): 4447–60. http://www.ncbi.nlm.nih.gov/pubmed/23160199 (August 13, 2017).

“Tick-Borne Encephalitis (TBE, FSME) Monograph.” 2007. http://www.tbe-info.com/upload/medialibrary/Monograph_TBE.pdf (August 14, 2017).

“Toll-Like Receptor Signaling Pathways: R&D Systems.” https://www.rndsystems.com/pathways/toll-like-receptor-signaling-pathways (August 7, 2017).

Vandesompele, Jo et al. 2002. “Accurate Normalization of Real-Time Quantitative RT-PCR Data by Geometric Averaging of Multiple Internal Control Genes.” *Genome biology* 3(7): RESEARCH0034. http://www.ncbi.nlm.nih.gov/pubmed/12184808 (August 13, 2017).

Vilibić-Čavlek, Tatjana et al. 2014. “[TICK-BORNE ENCEPHALITIS VIRUS: EPIDEMIOLOGICAL AND CLINICAL PICTURE, DIAGNOSIS AND PREVENTION].” *Acta medica Croatica : casopis Hravatske akademije medicinskih znanosti* 68(4–5): 393–404. http://www.ncbi.nlm.nih.gov/pubmed/26285473 (August 7, 2017).

Wengler, G, and G Wengler. 1989. “Cell-Associated West Nile Flavivirus Is Covered with E+pre-M Protein Heterodimers Which Are Destroyed and Reorganized by Proteolytic Cleavage during Virus Release.” *Journal of virology* 63(6): 2521–26.

http://www.ncbi.nlm.nih.gov/pubmed/2724410 (August 12, 2017).

Wu, Yaoxing et al. 2017. “Zika Virus Evades Interferon-Mediated Antiviral Response through the Co-Operation of Multiple Nonstructural Proteins in Vitro.” *Cell Discovery* 3: 17006. http://www.nature.com/articles/celldisc20176.

Yamamoto, Masahiro, and Kiyoshi Takeda. 2010. “Current Views of Toll-like Receptor Signaling Pathways.” *Gastroenterology research and practice* 2010: 240365.

Zhu, Jianzhong et al. 2014. “Antiviral Activity of Human OASL Protein Is Mediated by Enhancing Signaling of the RIG-I RNA Sensor.” *Immunity* 40(6): 936–48. http://dx.doi.org/10.1016/j.immuni.2014.05.007.

Zhu, Jianzhong, Arundhati Ghosh, and Saumendra N. Sarkar. 2015. “OASL - A New Player in Controlling Antiviral Innate Immunity.” *Current Opinion in Virology* 12: 15–19. http://dx.doi.org/10.1016/j.coviro.2015.01.010.